Journal of Hazardous Materials 475 (2024) 134900

Contents lists available at ScienceDirect

Journal of Hazardous Materials

journal homepage: www.elsevier.com/locate/jhazmat

Polylactic acid nanoplastics (PLA-NPLs) induce adverse effects on an *in vitro* model of the human lung epithelium: The Calu-3 air-liquid interface (ALI) barrier

Alba García-Rodríguez [a,1], Javier Gutiérrez [a,1], Aliro Villacorta [a,b], Jéssica Arribas Arranz [a], Iris Romero-Andrada [c], Alicia Lacoma [c], Ricard Marcos [a,*], Alba Hernández [a,*], Laura Rubio [a,*]

[a] Group of Mutagenesis, Department of Genetics and Microbiology, Faculty of Biosciences, Universitat Autònoma de Barcelona, Cerdanyola del Vallès, Spain
[b] Facultad de Recursos Naturales Renovables, Universidad Arturo Prat, Iquique, Chile
[c] Institut d'Investigació Germans Trias i Pujol, Badalona, Spain

HIGHLIGHTS

- An *in vitro* lung barrier containing Calu-3 cells has been set up.
- PLA nanoplastics were tested under short and long-term exposures.
- Easy internalization, tight-junctions, and mucus secretion effects were observed.
- Genotoxicity was induced mainly after lon-term exposures.
- Cellular proteins overexpression was induced mainly after long-term exposures

GRAPHICAL ABSTRACT

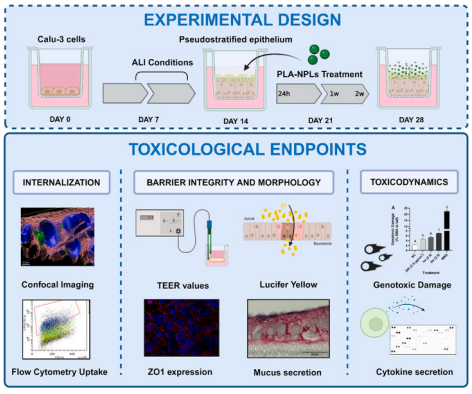

ARTICLE INFO

Keywords:
Nanoplastics
Polylactic acid
Callu-3 barrier
Long-term exposure
Air-liquid interphase

ABSTRACT

The expected increments in the production/use of bioplastics, as an alternative to petroleum-based plastics, require a deep understanding of their potential environmental and health hazards, mainly as nanoplastics (NPLs). Since one important exposure route to NPLs is through inhalation, this study aims to determine the fate and effects of true-to-life polylactic acid nanoplastics (PLA-NPLs), using the *in vitro* Calu-3 model of bronchial epithelium, under air-liquid interphase exposure conditions. To determine the harmful effects of PLA-NPLs in a more realistic scenario, both acute (24 h) and long-term (1 and 2 weeks) exposures were used. Flow cytometry results indicated that PLA-NPLs internalized easily in the barrier (~10 % at 24 h and ~40 % after 2 weeks), which affected the expression of tight-junctions formation (~50 % less *vs* control) and the mucus secretion (~50 % more *vs* control), both measured by immunostaining. Interestingly, significant genotoxic effects (DNA breaks)

* Correspondence to: Group of Mutagenesis, Department of Genetics and Microbiology, Faculty of Biosciences, Universitat Autònoma de Barcelona, Campus of Bellaterra, Cerdanyola del Vallès, 08193, Spain.
E-mail addresses: ricard.marcos@uab.cat (R. Marcos), alba.hernandez@uab.cat (A. Hernández), laura.rubio@uab.cat (L. Rubio).
[1] Both authors contributed equally.

https://doi.org/10.1016/j.jhazmat.2024.134900
Received 20 March 2024; Received in revised form 4 June 2024; Accepted 12 June 2024
Available online 13 June 2024

were detected by using the comet assay, with long-term effects being more marked than acute ones (7.01 *vs* 4.54 % of DNA damage). When an array of cellular proteins including cytokines, chemokines, and growth factors were used, a significant over-expression was mainly found in long-term exposures (~20 proteins *vs* 5 proteins after acute exposure). Overall, these results described the potential hazards posed by PLA-NPLs, under relevant long-term exposure scenarios, highlighting the advantages of the model used to study bronchial epithelium tissue damage, and signaling endpoints related to inflammation.

1. Introduction

Micro- and nanoplastics (MNPLs) can be considered as air pollutants. Recent studies have shown that these tiny plastic particles have become airborne and contribute to air pollution [8] being transported by the wind to great distances (and much faster than water). It is estimated that between 0.013 and 25 million tons of MNPLs are transported thousands of kilometers across countries, continents, and oceans each year by ocean air currents, snow, sea spray, or fog [2]. Therefore, besides ingestion, inhalation is one of the main routes of human exposure to MNPLs potentially affecting human health [47–49]. High concentrations of these emergent contaminants have been identified in both indoor (13,731 to 68,415 particles/y/capita) and outdoor (575 to 1008 MPLs/m^2/day) scenarios [12,62] and, as direct proof of human exposure, MNPLs have also been identified in the lungs of living individuals [30]. Despite the potential effects that MNPLs could trigger in the respiratory system, little is known about their interaction with pulmonary cells in the lung epithelia, and their possible effects on health. However, what it is well known is that particulate matter (PM), a mixture of particles existing in the air as contaminants (in the same way as MNPLs), has already been associated with premature mortality, cardiopulmonary diseases, asthma, chronic obstructive disease, pulmonary fibrosis, or lung cancer [36]. Based on the scarce data available on the potential effects of MNPLs in the respiratory system, it becomes urgent to invest efforts to decipher how these environmental particles interact with the lung barrier, and which are their adverse effects.

Although most of the studies devoted to determining the potential risks of MNPLs use petroleum-based plastics, there is a growing tendency to use “bioplastics”, made from biological materials. A Global Sustainable Development Report in 2015 from the United Nations stated that the increasing global awareness of sustainability is noticeably shifting consumer preferences. Accordingly, the industry must adapt to meet those preferences, along with the need for tools allowing the assessment of the environmental impacts of materials (UNDESA 2015). Therefore, as an alternative to petrol-based plastics, bio-based polymers are also used to produce huge amounts of disposable plastic goods [13]. Adverse effects (*e.g.*, intestinal damage, oxidative stress, DNA damage, inflammation, *etc.*) of their degradation products (MNPLs) have already been described pointing out that bioplastics have the potential to produce particles more rapidly, under certain conditions, due to its greater degradation capacity, compared with petroleum-based plastics (Kumar et al., 2023 and [1]).

Polylactic acid (PLA) is likely the most popular bio-based polymer and has been described to be: (i) eco-friendly since it is derived from renewable sources like corn, wheat, or rice, and can be recyclable and compostable; (ii) biocompatible as it is described non-toxic for local tissues; (iii) processable, as PLA has better thermal characteristics and can be processed by injection molding, thermoforming, giber spinning, *etc.*; and (iv) economically competitive because PLA requires 25 to 55 % less energy to produce than petroleum-based polymers [33]. Unfortunately, the terms biodegradable, recyclable, and composting used by manufacturers and distributors can be somewhat misleading for the final consumer, when it is not further defined. PLA can be recyclable and biologically degraded from a few days to a few months, but only under industrial composting conditions. In nature, however, it takes several years for PLA to decompose, which means that in aquatic and terrestrial environments it contributes to environmental plastic pollution. *In vitro* tests have shown that crystalline residues of PLA remain intact for over five years when placed in phosphate saline solution at physiological temperatures (37 ºC) [50,58].

Researchers and regulatory bodies are actively investigating the safety of bioplastics, but studies are just starting to unravel the potential health risks, associated with human exposure. By using *in vitro* and *in vivo* approaches we have shown that ingested PLA-NPLs can migrate from food packaging, internalize intestinal cells such as enterocytes and goblet cells, cross the protective mucus layer in the intestine, as well as the epithelial barrier, and interact with the gastrointestinal microbiota. Interestingly, the high internalization rate of PLA-NPLs induced an important genotoxic response [1,6]. Regarding *in vivo* studies, in growing mice PLA-MPL exposure induced more severe effects than those induced by polyvinyl chloride (PVC) MPLs [17], providing new insights for re-examining bioplastic safety. In addition, the *in vitro* digestion of PLA-MPLs generated nanoparticulated oligomers bioaccumulating in the liver, intestine, and brain of exposed mice, causing intestinal damage and acute inflammation [64]. Accordingly, our current hypothesis is that when inhaled, PLA-NPLs can exert detrimental effects on the respiratory system.

To decipher our hypothesis, we have established an *in vitro* lung epithelium model using the Calu-3 cell clone cultured in air-liquid interface (ALI) conditions. These conditions allow a bronchial representative cell differentiation resembling important physiological conditions of the lung barrier such as the expression of tight junctions, the formation of a polarized monolayer with mucociliary structures, the mucus secretion, and the formation of a solid and strong barrier stated by medium trans-epithelial electrical resistance (TEER) values [66]. The peculiarity of this ALI system consists of using a transwell membrane where cells grow connected by apical and basolateral compartments. In this layout, cells are fed with cellular liquid media through the basolateral compartment while maintaining an air phase in the apical side, which faithfully represents the air-cell contact of the lung’s anatomy. However, the most important trait of Calu-3 cells growing in ALI conditions is its long-term stability -more than 3 weeks after their establishment- [26]. Therefore, the main advantages of this *in vitro* model, when compared to those constructed with BEAS-2B or A549, are: tighter barrier conditions, differentiation of microvilli-like structures, more mucus production, longer experimental performance, and more relevant exposure scenarios in ALI conditions. In the present experimental context the effects of PLA-NPLs after acute (up to 24 h) and long-term conditions (up to 2 weeks) exposures were determined.

The study’s findings reveal significant insights into the impact of PLA-NPLs on bronchial epithelium tissue. Flow cytometry analysis demonstrated substantial internalization of PLA-NPLs within the barrier, leading to altered expression of tight junctions and increased mucus secretion. Remarkably, genotoxic effects were observed with long-term exposure resulting in more pronounced DNA damage, compared to acute exposure. Additionally, the proteome analysis revealed a significant over-expression, particularly in long-term exposures. These results underscore the potential hazards associated with PLA-NPLs, particularly under prolonged exposure conditions, emphasizing the importance of the utilized model in understanding bronchial epithelium damage and inflammatory signaling pathways.

2. Materials and methods

2.1. Obtention of PLA-NPLs and fluorescently-labelled PLA-NPLs

The PLA-NPLs were obtained using the top-bottom strategy, starting from commercial-grade polymers in the form of pellets. In this way, the obtained PLA-NPLs could be considered as true-to-life NPLs since the starting material contains plastic additives. The obtention procedure has already been published [1]. Briefly, a pre-mini emulsion was prepared by adding the aqueous phase consisting of dissolved Pluronic and polyvinyl alcohol (as co-stabilizer) in 120 mL of water (0.25 % wt and 2 % wt, respectively) to the organic phase composed of 1 g of PLA dissolved in 30 g dichloromethane and stirring magnetically for 60 min. Furthermore, ultrasonication under ice cooling was applied for 120 s at 80 % amplitude, and the obtained mini-emulsion was transferred to a round bottom flask to evaporate the organic solvent under pressure.

The fluorescently-labelled PLA-NPLs were obtained in the same way as the unlabeled PLA-NPLs (explained above) but a previous functionalization of PLA-NPLs was generated using a reactive extrusion, process without the use of solvents. Once PLA-NPLs were functionalized with amino groups, they were labelled by reacting with the fluorophore compound, 5' 6-FAM (fluorescein). For this purpose, 1 g of amino-functionalized PLA-NPLs was placed in a round-bottom flask provided with a magnetic stirring bar, an N_2 inlet, and a reflux condenser. Twelve milliliters of tetrahydrofuran were added under an inert atmosphere and, when the material was completely dissolved, 25 mg (2.5 % w/w) of a mix of 5-(and-6)-carboxyfluorescein and succinimidyl ester was added. The reaction mixture was stirred at room temperature and protected from light. After 1 h, water was added to precipitate the labelled PLA-NPLs (FAM-PLA-NPLs), which were filtered off, washed with water, and dried.

2.2. Physicochemical characterization of PLA-NPLs

The obtained PLA-NPLs were subjected to physicochemical characterization to determine shape, morphology, and degree of aggregation using scanning electron microscopy (SEM) (Zeiss Merlin, Zeiss, Oberkochen, Germany). For SEM investigation, PLA-NPLs suspension was loaded on the bright surface of cleaned silicon chips. Silicon chips were cleaned with drops of Milli-Q water and kept in a clean area. The average diameter of PLA-NPLs was determined by measuring 100 random particles of SEM images using ImageJ software. The presence of the characteristics functional groups of PLA particles was detected with Fourier transform infrared spectroscopy (FTIR) on a Hyperion 2000 system (Bruker Corporation, Billerica, 199 Massachusetts, USA). Finally, a Zetasizer® Ultra device from Malvern Analytical (Cambridge, United Kingdom) was used to evaluate the hydrodynamic size (by dynamic light scattering, DLS) and the total surface charge (Zeta potential) of PLA-NPLs (by laser Doppler velocimeter, LDV) in a water suspension. To determine the hydrodynamic size distribution of the individual particles in suspension, a combination of both Brownian movement and light scattering (Nano tracking analysis) was carried out in a Nanosight NS300 device (Malvern Panalytical Ltd, Cambridge, UK). The NTA technique is based on the tracking of single particles, whereas DLS measures a bulk of particles with a strong bias to the largest particle present in the sample [20]. Altogether highlights the importance not only of the use of complementary techniques but also of the number of particles to be analyzed.

2.3. The in vitro Calu-3 barrier, and the ALI model

The Calu-3 cell line was selected for the establishment of the *in vitro* lung epithelium barrier model since, after a differentiation time, can display epithelial morphology expressing tight junctions and secreting abundant mucous substances. Calu-3 cells are derived from human non-small-cell lung adenocarcinoma epithelial cells. Briefly, cells were cultured in Dulbecco's modified Eagle's high glucose medium (DMEM) (Biowest, France) supplemented with 10 % v/v fetal bovine serum (FBS), 1 % non-essential amino acids (NEA) 100x (Biowest, France) and 0.01 % Plasmocin™ (Invivo Gen, San Diego, CA). The 2D monocultures of Calu-3 were maintained in 75 cm^2 culture flasks at a density of 20,000 cells/cm^2 in a 5 % CO_2 humidified atmosphere at 37 ºC and weekly passaged before confluency. To create the bronchial epithelial barrier, 1 $\times$ 10^5 cells are seeded on 0.6 cm^2 polycarbonate transwell inserts with a pore of 0.4 μm (Millicell®, Merck) and covered with cell culture media in both basolateral (0.6 mL) and apical (0.4 mL) compartments. Culture media was replaced every two days.

To move to the air-liquid conditions, after 7 days of cell culturing, proliferation, and differentiation, the medium from the apical side was removed, leaving only 15 μL to moist the cells. At this point, the culture was extended for 7 more days changing the basolateral medium every day. After these 14 days, the epithelial barrier is considered fully established and differentiated (See Fig. 1).

2.4. Treatments with PLA-NPLs

To assess the effects of PLA-NPLs, the Calu-3 ALI system was exposed to different PLA-NPLs concentrations diluting the NPLs stock to the desired concentration and adding the minimum volume possible (15 μL) to the apical side. This treatment technique follows an internationally harmonized protocol, the PATROLS SOP (PATROLS SOP, 2022). Moreover, two exposure regimes, short-term (acute) and long-term (daily repeated for 1 and 2 weeks) were used. For acute exposures (lasting for 24 h), the concentrations of 2.5, 10, and 20 μg/cm^2 were used. For long-term repeated exposures, only the concentration of 2.5 μg/cm^2 was used (Fig. 1).

2.5. PLA-NPL's effects on the Calu-3 barrier function

To determine potential changes in the integrity, permeability, and functionality of the established epithelium, different assays and techniques were performed, as indicated below.

2.5.1. Trans-epithelial electrical resistance (TEER)

TEER is commonly evaluated as a parameter of the epithelium's integrity. Firstly, TEER values were measured using an epithelial volt-ohmmeter (Millicell-ERS) through the whole barrier formation process (every 3 days) and after its consolidation (day 14) to assess the barrier's basal stability. On day 14th the Calu-3 barrier was exposed to PLA-NPLs, and TEER measurements were done on day 15th, 21st, and 28th, after 24 h, 1 and 2 weeks of exposure, respectively. TEER values were calculated by subtracting the mean resistance of blank porous inserts (no-cells) from the mean resistance of inserts with cells and the treatments and multiplying by the surface area of the transwell insert (0.6 cm^2).

$$TEER = [\Omega \text{ (treated cell inserts)} - \Omega \text{ (cell-free inserts)}] \times 0{\cdot}6 \text{ cm}^2.$$

2.5.2. The Lucifer yellow assay

The denominated paracellular permeability is an important property to cover when assessing the correct establishment of an *in vitro* epithelial barrier and its proper functionality as a barrier. The paracellular permeability is conditioned by the establishment of the epithelial cell tight junction structure, which regulates the crossing of solutes and water between epithelial cells. To analyze how permeable is a barrier we used Lucifer yellow (LY), which is a small fluorescent hydrophilic molecule that only crosses the barrier through passive paracellular diffusion. The LY assay was used to follow the permeability after exposing the 14-days-old Calu-3 barrier to the different concentrations (2.5, 10, and 20 μg/cm^2) of PLA-NPLs at acute (24 h) and long-term

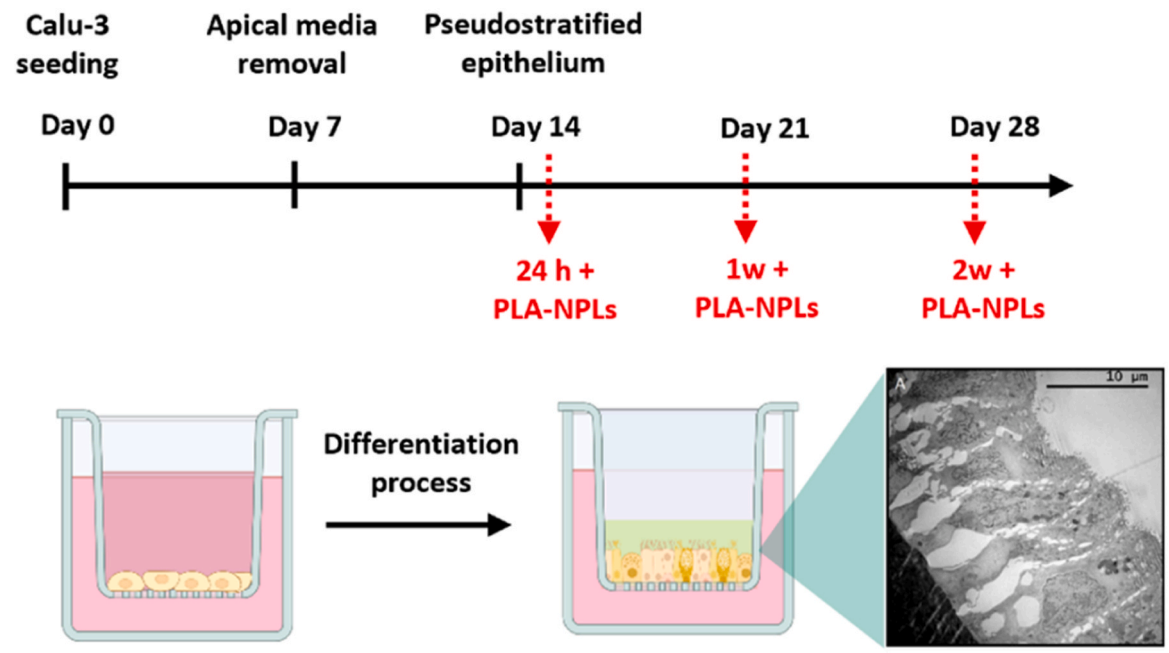

Fig. 1. Experimental design. Graphical representation and time-course of Calu-3 barrier formation, differentiation, and exposure (24 h, 1 week, and 2 weeks) to PLA-NPLs.

exposure (1 and 2 weeks). Briefly, after the treatments, barriers were washed three times with Hank's Balanced Salt Solution (HBSS; Ca^{2+}, Mg^{2+}, +10 mM HEPES, pH 7.4), a transport buffer. The inserts were then transferred to a new 24-well plate with 0.5 mL of HBSS in the basolateral compartment and LY (0.5 mg/mL) diluted in HBSS was also added to the apical compartment. The plates were left at 37 ºC for 2 h. Later, 100 µL of each basolateral compartment was transferred in triplicates to a black 96-well plate. Finally, the crossed LY was measured in a prompt fluorimeter (Victor III, Perkin Elmer) plate reader using a 405–535 nm excitation-emission spectrum. As a positive control, benzalkonium chloride (BNZ, 20 mg/mL, Sigma Aldrich) was used, as an agent able to denature tight junctions and permeate the barrier.

2.5.3. Identification of tight junctions (ZO-1) by immunostaining

To directly measure the effects of PLA-NPLs on the epithelium's tight junctions, an immunofluorescence staining was carried out to visualize and quantify the expression of zonula occludens-1 protein (ZO-1). Briefly, after the acute (24 h) and long-term exposures (2 weeks), cells were washed with PBS 1x and then fixed with ice-cold 4 % paraformaldehyde (PFA) (Santa Cruz Biotechnology (Dallas, TX, USA) for 10 min, washed twice with cold PBS, and then permeabilized with 0.1 % Triton X-100 (Merk, Darmstadt, Germany) for 15 min at room temperature in a humidified chamber. After washing twice with PBS, bovine serum albumin (BSA) 2 % w/v in PBS was used to block for 30 min. The primary antibody, rabbit anti-ZO-1 antibody (Abcam, Cambridge, MA, USA), was diluted (1/200) in 1 % w/v BSA in PBS, and the cells were then incubated with the diluted antibody overnight at 4 °C. The secondary antibody, anti-rabbit IgG 647 nm-conjugated antibody (Thermo Fisher Scientific, Waltham, MA, USA), was diluted (1/250) in 1 % BSA in PBS, and the cells were then incubated in the diluted antibody solution for 2 h at 37 °C. The transwell membranes were excised with a scalpel from the inserts and mounted in VECTASHIELD Antifade Mounting Media (Vector Laboratories, Burlingame, CA, USA). A Leica TCS SP5 (Leica Microsystems GmbH, Mannheim, Germany) laser confocal microscope was used to analyze ZO-1 fluorescence intensity. To stain the cell nucleus, and thus define individual cells, Hoechst 33342 (ThermoFisher Scientific, Waltham, MA, USA) was used with a maximum excitation/emission of ~405/425–475 nm diluted in DMEM culture media at a concentration of 1/500 for 15 min

2.5.4. Histochemical identification of the barrier's mucus secretion

The secretion of mucus is a property of the Calu-3 cell line under ALI conditions, which is essential to resemble the microenvironment of the native lung epithelium containing the extra protective layer of mucins. Hence, we aimed to assess the effects of PLA-NPLs on the mucus layer using Alcian Blue as histochemical staining. Alcian Blue is a cationic dye commonly used in histology and cytology to stain acidic mucins since is attracted due to its positively charged nature. Briefly, after the exposures, the Calu-3 epithelium was fixed with 4 % paraformaldehyde (PFA) (Santa Cruz Biotechnology, Dallas, TX, USA) for 30 min and stained with Alcian Blue (pH 2.5) (Abcam, Cambridge, UK) for 30 min. After washing the samples with distilled H_2O for 1 min, the cell barriers were excised from their supports, and cross-sections of 3 to 5 µm were obtained with a microtome and fixed in microscope slides. Sample images were randomly obtained with an inverted light Axio Observer A1 microscope (Zeiss, Oberkochen, Germany) complemented with an AxioCam MRm camera (Zeiss, Oberkochen, Germany).

2.6. Toxicokinetic analysis

To specifically understand how PLA-NPLs interact with and move within the *in vitro* Calu-3 barrier, as well as the absorption and distribution of such nanoparticles, flow cytometry and confocal microscopy were used. To such end, the fluorescently labelled PLA-NPLs (FAM-PLA-NPLs) were used at the same concentration (2.5, 10, and 20 µg/mL) to expose acute (24 h) and chronically (1 and 2 weeks) the *in vitro* lung epithelia. Briefly, after the exposure, cells were washed 3 times with 1X PBS (0.1 M) to remove the excess of FAM-PLA-NPLs, trypsinized with trypsin-EDTA 1 % for 5 min, and resuspended in 5 mL tubes to analyze the cell internalization using the CytoFELX FACS from Bechman Coulter (Pasadena, CA, USA). The internalization of nanoplastics was detected with an excitation-emission spectra of 488–525 nm. With this approach, the absolute number of cells containing enough FAM-PLA-NPLs to be detected was determined and expressed as the percentage of cells that have internalized nanoplastics.

To corroborate the exact location of FAM-PLA-NPLs, a laser confocal

microscopy Leica TCS SP5 (Leica Microsystems GmbH; Mannheim, Germany) device was used. For that, after the acute and long-term exposures to FAM-PLA-NPLs, Calu-3 cells were washed with 1X PBS, fixed with ice-cold 4 % paraformaldehyde (PFA) (Santa Cruz Biotechnology (Dallas, TX, USA) for 10 min, washed twice with cold PBS, permeabilized with 0.1 % Triton X-100 (Merk, Darmstadt, Germany) for 15 min at room temperature, and incubated with bovine serum albumin (BSA) 2 % w/v in PBS for 30 min. The staining with ZO-1 was used to visualize the cell membrane perimeter. To such end, cells were incubated with rabbit anti-ZO-1 (1/200) overnight at 4 °C. After washing steps with 1X PBS, the secondary antibody, anti-rabbit IgG 647 nm-conjugated antibody (1/250), was left for 2 h at 37 °C. The transwell membranes were excised with a scalpel from the inserts and mounted in VECTASHIELD Antifade Mounting Media containing Hoechst 33342 (Vector Laboratories, Burlingame, CA, USA). Finally, the z-stacks were processed using the Fiji extension of Image J software and Imaris Microscopy Image Analysis Software v. 9.6 from Oxford Instruments (Abingdon, England).

2.7. PLA-NPLs effects on the Calu-3 barrier toxicological profile

Several endpoints including NPLs uptake and toxicokinetic studies, production of intracellular reactive oxygen species (ROS), genotoxic and oxidative DNA damage, as well as inflammation and cytokine production were assessed to describe the toxicological profile of PLA-NPLs on the *in vitro* Calu-3 barrier model.

2.7.1. Genotoxic and oxidative DNA damage

The alkaline comet assay, also known as the single-cell gel electrophoresis assay, was used to evaluate the levels of genotoxic damage, specifically DNA breaks, after the *in vitro* Calu-3 barriers were acutely (24 h) and chronically (1 and 2 weeks) exposed to different concentrations of PLA-NPLs (2.5, 10, and 20 μg/mL). Moreover, the addition of FPG (formamidopyrimidine DNA glycosylase) permits the study of oxidative damage in the DNA bases. This enzyme specifically recognizes DNA lesions such as 8-oxoguanine, which is a common oxidative DNA lesion generated by ROS. The experiment also included a negative (untreated samples) and two positive controls: (i) methyl methanesulphonate (MMS) as a genotoxic agent (200 μM for 30 min at 37 ºC) and (ii) potassium bromate ($KBrO_3$) as oxidative agent (5 mM for 30 min at 37 ºC). Briefly, after the exposure cells were washed 3x with 1X PBS, detached with trypsin-EDTA 1 %, and the trypsin inactivated with inactivator (2 % FBS diluted in 1x PBS). Cells were collected, centrifuged for 5 min at 150x g at 4 ºC, and resuspended in cold PBS to a final concentration of 1 × 10 cells/mL. Cells were then mixed with 0.75 % low melting point agarose at 37 ºC and drops of 10 μL of each treatment were dropped on Gelbond films (GBFs) in duplicates. GBFs were left overnight in lysis buffer (4 ºC), washed in electrophoresis buffer for 5 min, and incubated with fresh electrophoresis buffer for 35 min at 4 ºC to allow DNA unwinding. Following, the electrophoresis was done at 20 V/300 mA for 20 min at 4 ºC. A series of washes with PBS and distilled water were performed before the cell fixation with absolute ethanol for 1 h. Finally, the staining of cells was done using SYBER™ Gold (1:10000) in TE buffer for 20 min at room temperature in agitation. The results were visualized using an Olympus BX50 epifluorescence microscope (Olympus; Tokyo, Japan) at 20X magnification. The DNA damage was analyzed with the Komet 5.5 image software (Kinetic Imagin Ltd; Liverpool, UK) as the percentage of DNA in the tail. Approximately 100 cells, randomly selected, were analyzed per drop.

2.7.2. Proteome array and cytokine release analysis

The Human XL Cytokine Array Kit (USA R&D Systems, Inc), a proteome profiler array, was used to measure the relative expression levels of soluble cellular proteins including cytokines, chemokines, and growth factors after treating the *in vitro* Calu-3 barrier to different concentrations of PLA-NPLs at different time points (24 h, 1, and 2 weeks). Briefly, the apical media (cell culture supernatant), where the extracellular signaling molecules might have been released after the treatments, were collected and stored at − 20 ºC for further experimentation. Then, a nitrocellulose membrane containing 105 different capture antibodies printed in duplicate was incubated with the collected medium at 4 ºC overnight. Later, the membrane was washed to remove the excess material and incubated with a mix of biotinylated detection antibodies. For detection, a streptavidin-HRP and chemiluminescent reagents are used, as indicated by the manufacturer. Finally, a signal is revealed at each capture spot corresponding to the amount of protein-bound, which can be analyzed using Image J. Results were imported to STRING Database to generate functional cytokines association networks, as previously described [5].

2.8. Statistical analysis

The obtained data were the average of at least two experiments containing duplicates per treatment. Data analysis was performed using GraphPad Prism 9 software (GraphPad Software Inc., CA, USA). To test the normal distribution of the data, the Shapiro-Wilk test was used, followed by the one-way ANOVA with Tukey's multiple comparisons test as a parametric test, or the Kruskal-Wallis test as a non-parametric one. Statistical significance was depicted as * $p \leq 0.05$, * * $p \leq 0.01$ and * ** $p \leq 0.001$.

3. Results and discussion

To date, most of the pulmonary toxicodynamic studies of MNPLs have been carried out using conventional and simplistic *in vitro* models such as undifferentiated cell cultures, including both A549 human alveolar type II-like epithelial and BEAS-2B human bronchial epithelial cells [10]. *In vivo* mouse models have also been used for MNPL exposures. However, it has been repeatedly shown that animal models may not be suitable enough for the exhaustive testing of the immense variety of existing types of polymeric particles (chemical origin, size, shape, additives, functionalization, *etc.*) [52]. It is important to emphasize that most of the investigations have focused on the toxicity of pristine polystyrene (PS)-MNPLs -used as reference material- either comparing different sizes or surface functionalization. This is mostly because of the lack of other commercially available MNPLs, more relevant from an environmental point of view, for research purposes [63]. Thus, although obtaining true-to-life MNPLs resulting from the laboratory degradation of plastic goods is a challenge this is the correct way to estimate the real risk associated with the exposure to the environmental secondary MNPLs.

Herein, we aimed to escape from simplistic methodological approaches acknowledging that the bronchial epithelium is one of the main protective barriers in the human lungs being constantly and chronically exposed to airborne MNPLs. Thus, Calu-3 barriers in ALI conditions were acutely and long-term exposed to different concentrations of PLA-NPLs, a widely produced biodegradable polymer utilized as a potential alternative to petroleum-based plastics [37]. The used PLA-NPLs (resulting from pellet degradation) can be considered a true-to-life particulate material environmentally relevant since it has been recently demonstrated their leachate from consumer products like teabags, plastic cutlery, and 3D printers [6,70].

3.1. PLA-NPLs characterization

The PLA-NPLs used in this study are derived from the degradation of PLA pellets as stated in our previous works [1]. Therefore, to have a clear profile of our material we thoroughly characterized the PLA-NPLs morphology, size distribution, hydrodynamic size, stability, surface charge, and chemical composition (Fig. 2). As observed by SEM, nanoparticles showed a spheric-like geometry in all cases (Fig. 2a). An average value of 130.06 nm was calculated from more than 1000

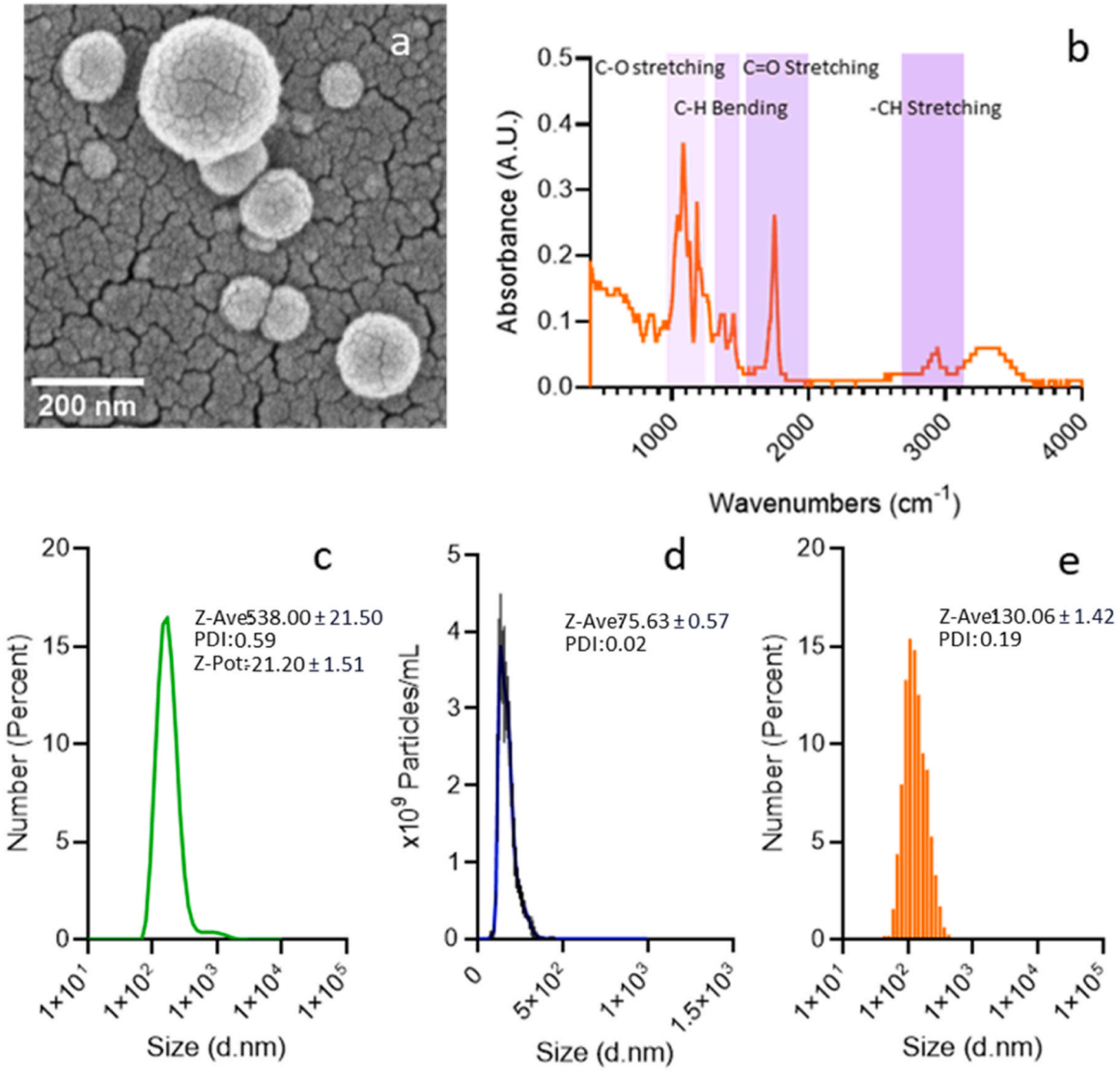

Fig. 2. PLA-NPLs characterization. (A) SEM image of PLA-NPLs. (B) FTIR Spectra of PLA-NPLs showing the distinctive chemical bounds for the bio-polymer. (C) Hydrodynamic size, PDI, and Z-potential of PLA-MNPLs measured by DLS. (D) Particle concentration, hydrodynamic size, and PDI of PLA-NPLs by NTA. (E) Primary particle size (Martin diameter) of PLA-NPLs measured from SEM images using ImageJ.

particles, measured for Martin diameter determination, and a polydispersity index (PDI) of 0.19 was calculated. When the hydrodynamic behavior (DLS) and surface interaction charge (Z-potential) were determined, the resulting hydrodynamic size value was 538.00 nm (Fig. 2c). This increase in average size when the particles are in suspension is highly related to the PDI which also increased to 0.59, suggesting a potential particle aggregation. The Z-potential value was consistently close to the average value of − 21.20 mV, which is reflected in the low standard error (SE) value of − 1.51, indicating a relatively stable suspension. These results agree with our previous publication where the hydrodynamic size and Z-potential of PLA-NPLs in water suspension averaged 425.7 nm and − 16.2, respectively [1]. To further investigate the behavior of PLA-NPLs in suspension, the nanoparticle tracking analysis (NTA) -a combination of Brownian movement and light scattering analysis- was also utilized. NTA determined a rather narrower size distribution of the PLA particles with an average value of 75.63 nm and a PDI of 0.02 (Fig. 2d). This phenomenon has been previously reported, where NTA values were always smaller than the DLS ones when measuring either polymer or metal oxide nanoparticles (Garcia-Rodríguez et al., 2022; [6]). Finally, the Fourier transform infrared spectroscopy analysis demonstrated the chemical identity of the used PLA-NPLs. The common PLA peaks for stretching frequencies for C═O are found at 1746 cm^{-1}, asymmetric and symmetric -CH3 stretching marker on the 2940 to 3000 cm^{-1} region, and C-O stretching at 1080 cm^{-1}. In addition, characteristics -CH3 asymmetric and symmetric bending bands were identified in 1452 and 1361 cm^{-1}, respectively (Fig. 2b).

3.2. PLA-NPLs toxicokinetic. Adhesion, adsorption, and fate

The ability of MNPLs, specifically PS-NPLs, to internalize into different cell types including epithelial cells (like Caco-2, HT29, and BEAS2-B), and hematopoietic cells (like THP-1, Raji-B, and TK6), independently on size and functionalization (pristine, amino-, and carboxylated-NPLs) has been extensively reported [18,57]. In addition, the formation of a bio-corona (adhesion of different biomolecules to the particle's surface) is a driving factor that increases PS-NPLs cell uptake as well as its toxic effects ([62]; Brower et al., 2024). Therefore, using two well-complemented techniques such as flow cytometry and confocal microscopy we have monitored the bio-interactions of FAM-PLA-NPLs with the *in vitro* bronchial epithelium Calu-3 barrier.

As depicted in Fig. 3, FAM-PLA-NPLs internalization into Calu-3 cells

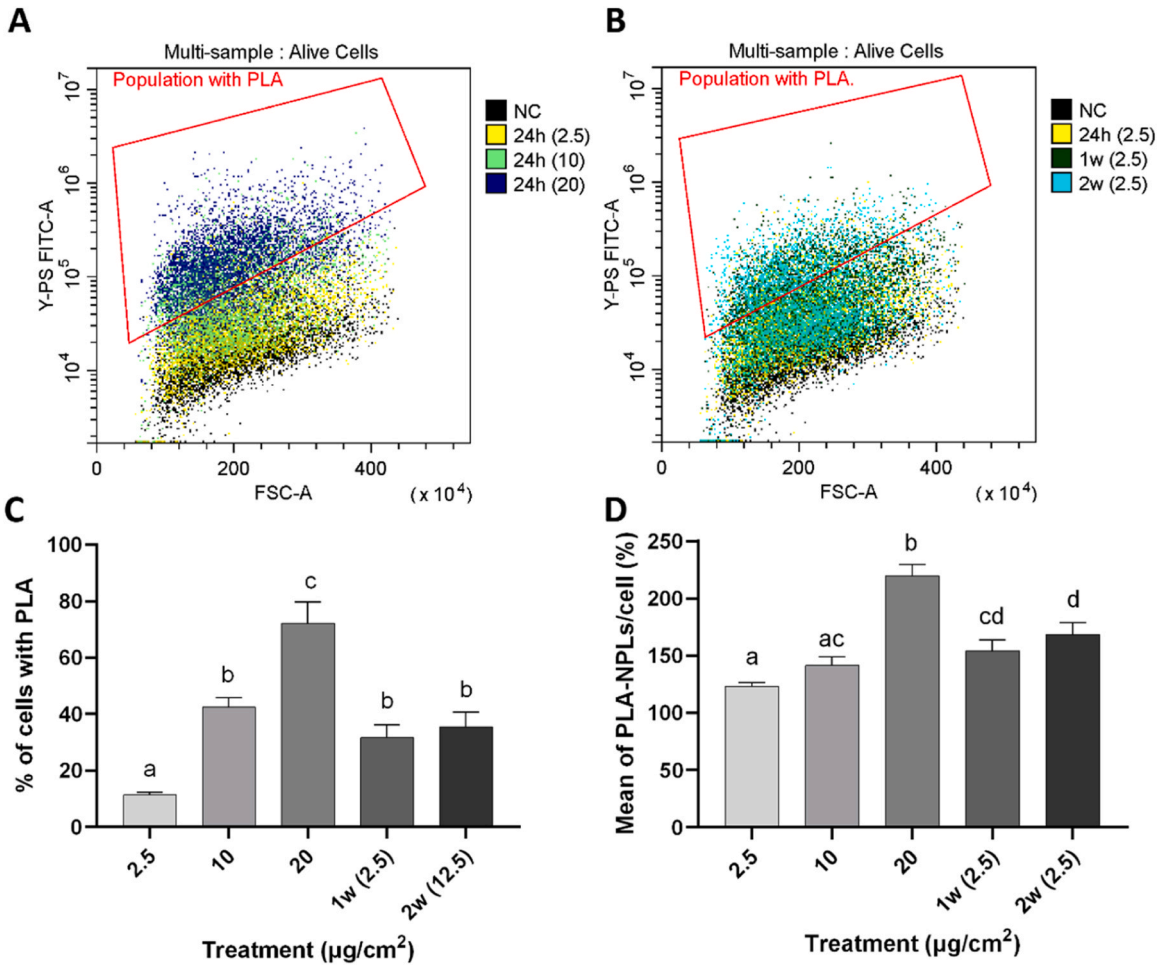

Fig. 3. Cell internalization of PLA-NPLs. (A) CytoFLEX plot representing the population of cells with FAM-PLA-NPLs (inside the red box) after exposing Calu-3 barriers to 2.5, 10, and 20 µg/cm^2 for 24 h. (B) CytoFlex plot indicating the cell population with FAM-PLA-NPLs after 24 h, 1, and 2 weeks of exposure with 2.5 µg/cm^2 PLA-NPLs. (C) Percentage of cells that contain FAM-PLA-NPLs, regarding each treatment. (D) Amount of internalized FAM-PLA-NPLs per cell. Data are expressed as mean ± SEM and analyzed with the one-way ANOVA with the multiple comparisons Dunnett's post-test. All those bars that do not share any letter are significantly different at $p \leq 0.05$. The NC columns, as unexposed cells, are not indicated in C and D because their values are zero.

was concentration-dependent (2.5 µg/cm^2 = 10 %; 10 µg/cm^2 = 40 %; and 20 µg/cm^2 = 70 % of internalized cells) (Fig. 3C). On the other side, when Calu-3 barriers were long-term exposed to 2.5 µg/cm^2 of FAM-PLA-NPLs for 1 and 2 weeks, the internalization rate was maintained at 30–35 %. Interestingly, the same accumulative tendency for different PS-NPLs (carboxylated-PS 20 and 200 nm, aminated- and pristine-PS 200 nm) was observed in Calu-3 barriers exposed for 28 days [40]. Using monocultures of human intestine-derived epithelial cells like Caco-2 and HT29, the rate of PLA internalization was significantly different between cells. Thus, while after 24 h 100 % of HT29 cells internalized at least 1 particle of PLA, the internalization in Caco-2 cells plateaued at 70 % after 48 h [6]. When calculating the mean fluorescent intensity per cell (nº of PLA-NPLs/cell), no significant differences in the number of internalized particles per cell after 2.5 and 10 µg/cm^2 exposures were observed neither comparing 1 *versus* 2 weeks of long-term exposure (Fig. 3D). It should be noted that Figs. C and D do not contain a negative column since, as unexposed cells, no fluorescent PLA-NPLs were internalized. These results would suggest (i) that human epitheliums can distinctly modulate/regulate the transient uptake and passage of different particulate material (*i.e.*, polymer type, size, and surface functionalization), according to the epithelium origin or cell type function; and (ii) that epitheliums actively work to balance the tissue homeostasis. Overall, the *in vitro* bronchial epithelium Calu-3 shows remarkable plasticity and endurance upon long-term exposures to NPLs.

Complementing the above-mentioned findings, Fig. 4 shows the images taken with confocal microscopy after exposure to 2.5 µg/cm^2 FAM-PLA-NPLs for 24 h and 2 weeks. This technique permits the 3D recreation of the tissue structure and the spatial localization of the particles (green). Accordingly, already at 24 h, it is observed how particles are inside the cell cytoplasm, close to the nuclear membrane (Fig. 4E), and in some cases inside the nucleus compartment (Fig. 4H). Similarly, after 2 weeks of exposure, barriers were found still containing severe nucleus-particle interactions (Figs. 4F and 4I), which can eventually lead to some sort of DNA damage and their consequent genotoxic effects. It must be noted that nanoparticles of polylactic-co-glycolic acid (PLGA), mainly used in drug delivery studies, and with similar PLA`s physicochemical characteristics, have also been reported to rapidly internalize and accumulate in Calu-3 cells, especially around the nuclei, but with no reported toxicity [42,65]. In addition, an identical trend was described when exposing the *in vitro* model Caco-2/HT29 (an intestinal epithelium simulation) to teabags-derived PLA-NPLs, where immediately after 24 h several cells showed nucleus-PLA interactions [6]. Using *in vivo* models, not only epithelial intestinal cells (enterocytes) internalized PLA-NPLs, but also bacteria of the larvae's midgut lumen from *D. melanogaster* showed a great internalization of that bio-polymer [1].

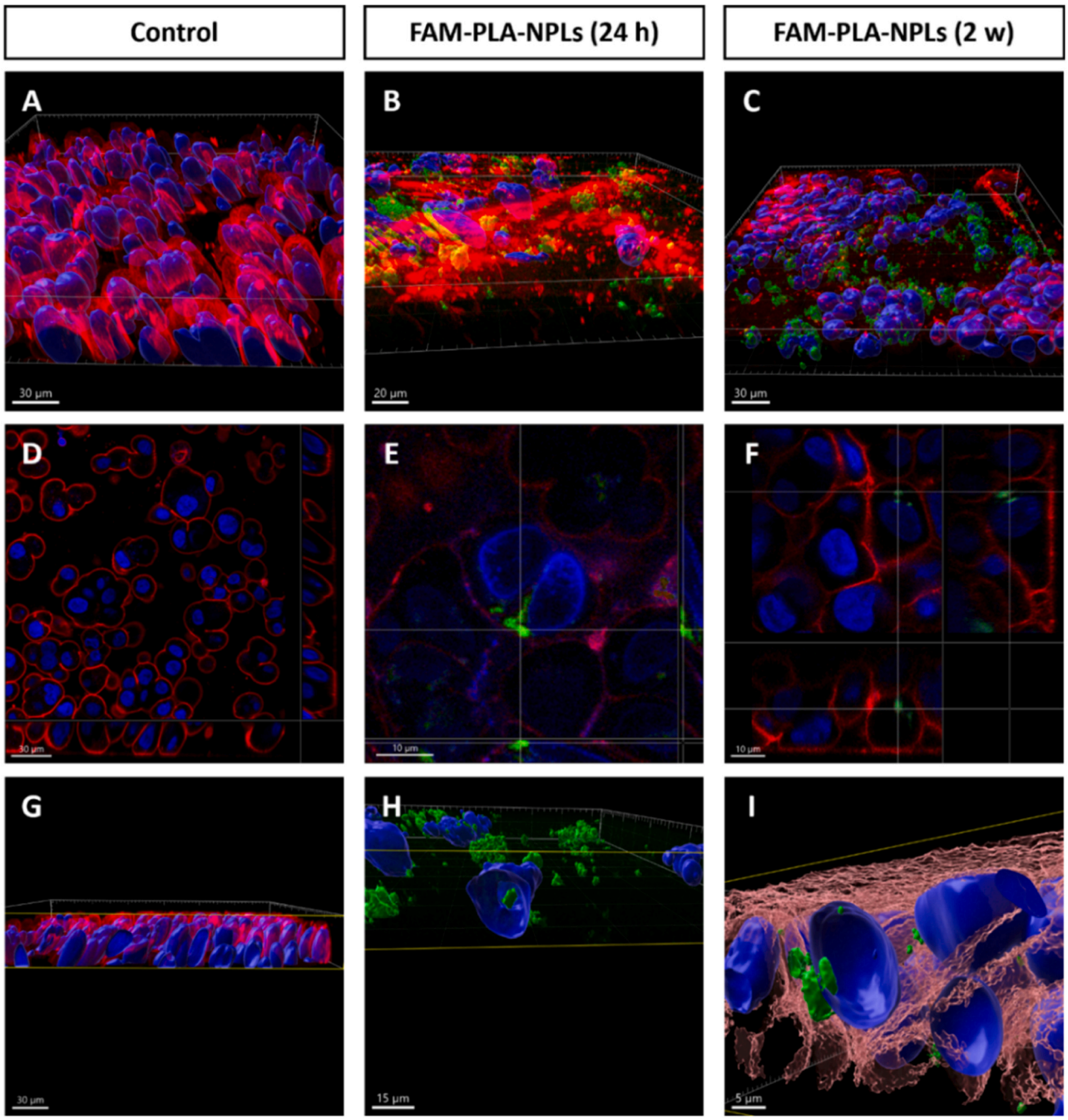

Fig. 4. Confocal images of PLA-NPLs internalization. (A-C) 3D images of Calu-3 barriers untreated and treated to PLA-NPLs for 24 h and 2 weeks, respectively. (D-E) Orthogonal views demonstrating the presence of PLA-NPLs inside the cell cytoplasm. (G-I) 3D images with cross-sectional views demonstrating the presence of PLA-NPLs in the nuclear compartment. PLA-NPLs, cell nuclei, and ZO-1 junctions are seen in green, blue, and red, respectively.

3.3. PLA-NPLs effects on the barrier structure and functionality

Overall, the respiratory airways play a critical role in maintaining the health and function of the lungs by protecting them from harmful substances, facilitating the clearance of mucus and particles, and helping to regulate airflow and gas exchange. More specifically the bronchial epithelium represents the most compact and highly organized tissue, constituting an impermeable epithelial barrier of the human body. The bronchial epithelium is arranged in a pseudostratified orientation with all cells contacting the basement membrane but only some reaching the luminal surface, where the ciliary structures are facing and everything is protected by an extra layer (approximately 30 μm) of mucus [7].

Repeated injury, repair, and regeneration of the airway epithelium following exposure to environmental factors and inflammation, results in histological changes and functional abnormalities in the airway mucosal epithelium (Gon et al., 2018). Hence, we have also monitored the structural rearrangements and the barrier permeability by measuring changes in the TEER values and in the paracellular passage of LY, respectively. As shown in Fig. 5, the presence of PLA-NPLs did not produce significant changes in the TEER values at any of the evaluated exposure conditions, nor time exposure regimes (acute *vs* long-term) (Fig. 5A and B). When benzalkonium (BNZ, 20 mg/mL) was used as a positive control (PC), a very significant decrease in TEER values was observed, confirming the goodness of the performed assay. In a similar work, exposures to PLA-NPLs (100 μg/mL) up to 72 h did not disrupt the barrier integrity of the *in vitro* intestinal barrier Caco-2/HT29 model [6].

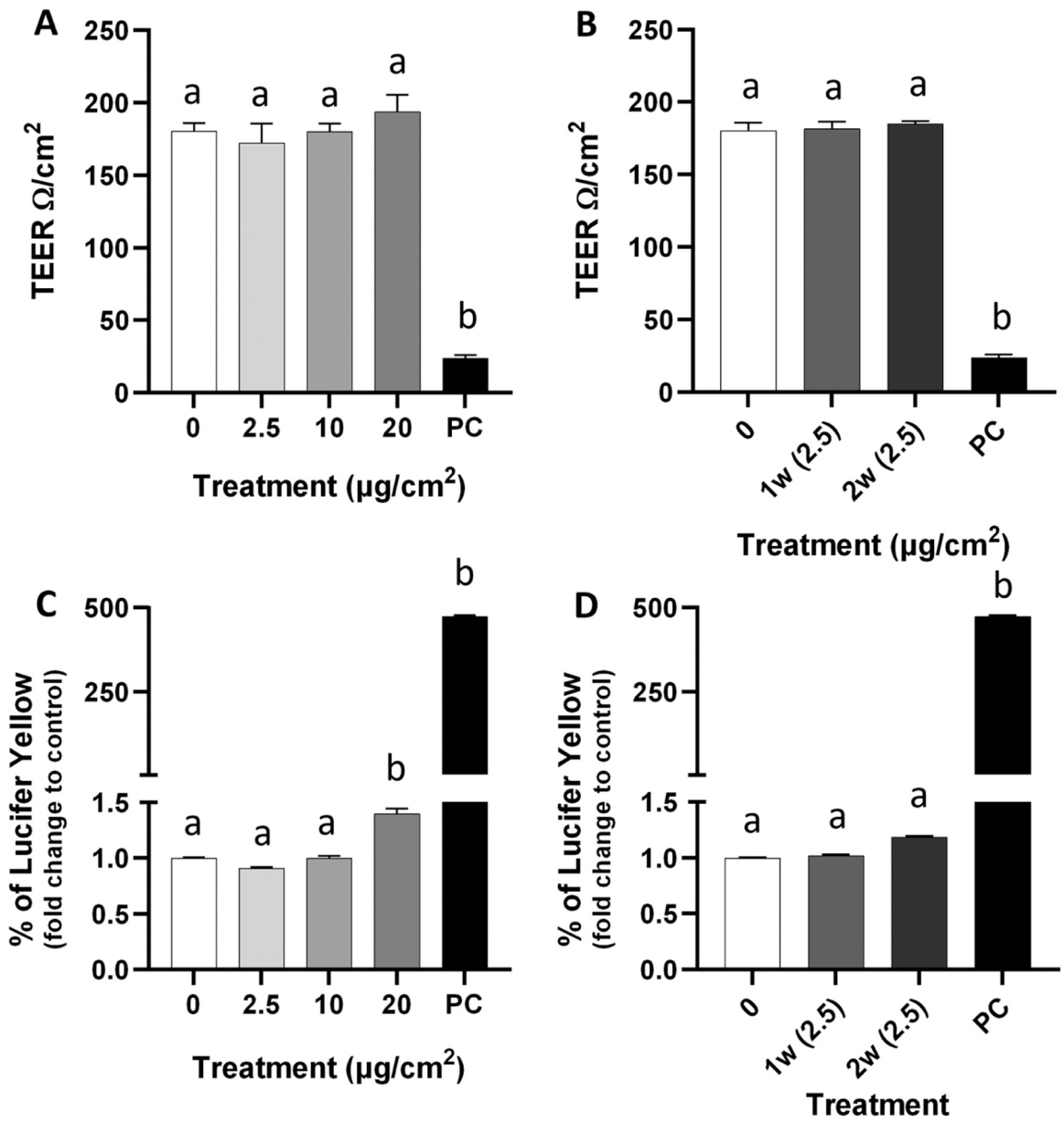

Fig. 5. Effects of PLA-NPLs on the integrity of Calu-3 barrier. (A) TEER values after acute (2.5, 10, 20 µg/cm^2) exposure to PLA-NPLs. (B) TEER values after long-term (2.5 µg/cm^2) exposures to PLA-NPLs. (C) Lucifer yellow permeability after acute exposures to PLA-NPLs. (D) Lucifer yellow permeability after long-term exposures to PLA-NPLs. Data represented as mean ± SEM and analyzed using the t-test. All those bars that do not share any letter are significantly different at $p \leq 0.05$.

To our knowledge, only a few investigations have studied the hazardous effects of PLA-NPLs in the respiratory airways using *in vitro* barrier models. Although not using specifically PLA-NPLs, no alterations in the TEER values were found after exposing Calu-3 barriers (in ALI conditions) to 200 µg/mL PLGA/PVA- and PLGA/PF68-NPLs for 24 h [43]. Similarly, exposing Calu-3 and A549 barriers to 2 µg/cm^2 of differently functionalized polystyrene (PS-NPLs) (20 and 200 nm), no significant changes in the barrier's integrity were observed [40]. On the other hand, by exposing an alveolar epithelial barrier in combination with endothelial cells (HPAEpiC/HUVEC) to PS-NPLs, significantly decreased TEER values were observed at all the concentrations tested (7.5, 15, and 30 µg/cm^2) in exposures lasting for 24 h [69].

The effects on the barrier's permeability were also determined. As depicted in Fig. 5C, the highest concentration (20 µg/cm^2) in the acute (24 h) exposure conditions showed a significant increase in the Calu-3 barrier permeability, indicating epithelial damage and most probably cytotoxicity. Thus, for the following assays only the 2.5 µg/cm^2 concentration was selected as a subtoxic dose and for a relevant long-term exposure.

Both TEER and LY assays have been extensively used as conventional techniques to measure barrier stability. However, they are not sensitive enough for pseudostratified epitheliums. Hence, the immunostaining of junctional proteins as ZO-1 was also performed after exposing Calu-3 barriers to 2.5 µg/cm^2 for 24 h and 2 weeks (Fig. 6). As observed (Fig. 6D), a significant decrease in ZO-1 was detected when compared to the negative control. Similar effects were also detected, by western blot in A549/HUVEC barriers exposed to 40 nm PS-NPLs for 24 h [69]. It is worth mentioning that A549 barriers are morphologically and structurally different from Calu-3 barriers, as the first ones do not form a pseudostratified epithelium nor differentiate into columnar-ciliated cells, which indicates the high sensitivity of A549 to exogenous exposures. Other studies have also identified different sensitivities to nanoparticles when working with advanced ALI lung models, depending on the used cell line and the treatment [19]. For example, alterations in the

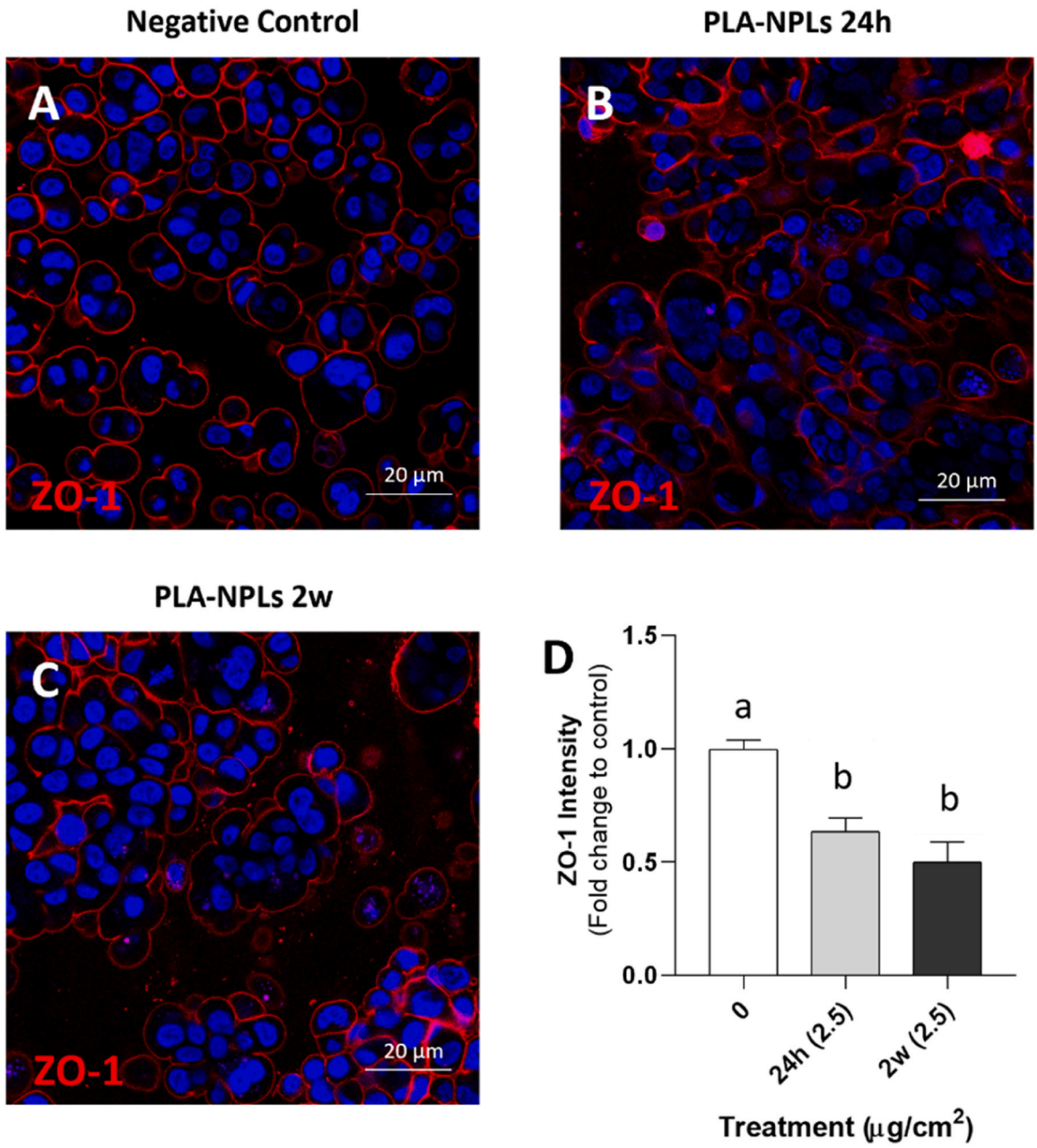

Fig. 6. Immunostaining of tight junction. (A-C) Representative confocal images of untreated, and 24 h and 2 weeks treated Calu-3 barriers with 2.5 µg/cm^2 PLA-NPLs. In blue the cell nuclei and in red the tight junction ZO-1. (D) Analysis of the ZO-1 intensity by ImageJ. Data was expressed as mean ± SEM and analyzed with one-way ANOVA with multiple comparisons Dunnett's post-test. All those bars that do not share any letter are significantly different at $p \leq 0.05$.

expression of ZO-1 and occludin were found after exposing the co-culture of 16HBE/THP-1/HLMVEC (mimicking an airway epithelium) to 128 µg/mL graphene and graphene oxide up to 24 h [61]. At this point, it is important to remark that the smaller the NPs the higher the ability to penetrate cell-to-cell spaces, disrupting tight junctions' molecules, and starting an epithelium remodeling cascade [54].

Another important aspect of pulmonary airway physiology requiring special attention is the biological hydrogel (known as mucus) forming a protective barrier for the underlying epithelium. The human pulmonary mucus is a viscoelastic hydrogel with a complex composition and molecular structure that humidifies and lubricates the airways, playing a protective and defensive role by entrapping exogenous particulate material as well as pathogens, helping their clearance through the mucociliary elevator *via* coordinated movement of ciliated apical airway epithelial cells [28,41]. The impairment or dysfunction of mucus in the respiratory tract can have significant consequences on respiratory health, including reduced airway clearance, chronic respiratory infections, airway inflammation, exacerbation of underlying conditions, and decreased overall lung function [28]. Accordingly, we assessed changes in the mucus content after exposing Calu-3 barriers to 2.5 µg/cm^2 PLA-NPLs for 24 h and 2 weeks (Fig. 7). For that purpose, we used Alcian blue staining, a dye that selectively binds to acidic mucins (the major component of the mucus). Although the results were not statistically significant (one-way ANOVA; $p = 0.0774$), mucus secretion tended to increase after long-term exposure to PLA-NPLs (approximately 50 % more) (Fig. 7D). Using this barrier model, the glycoproteins in the apical secretome of Calu-3 barriers exposed to Ag-NPs (10 µg/cm^2) significantly decreased after exposures lasting for 3 and 4 days, independently of the mRNA expression of MUC5AC [14]. Utilizing another common *in vitro* barrier (the intestinal barrier Caco-2/HT29-MTX)

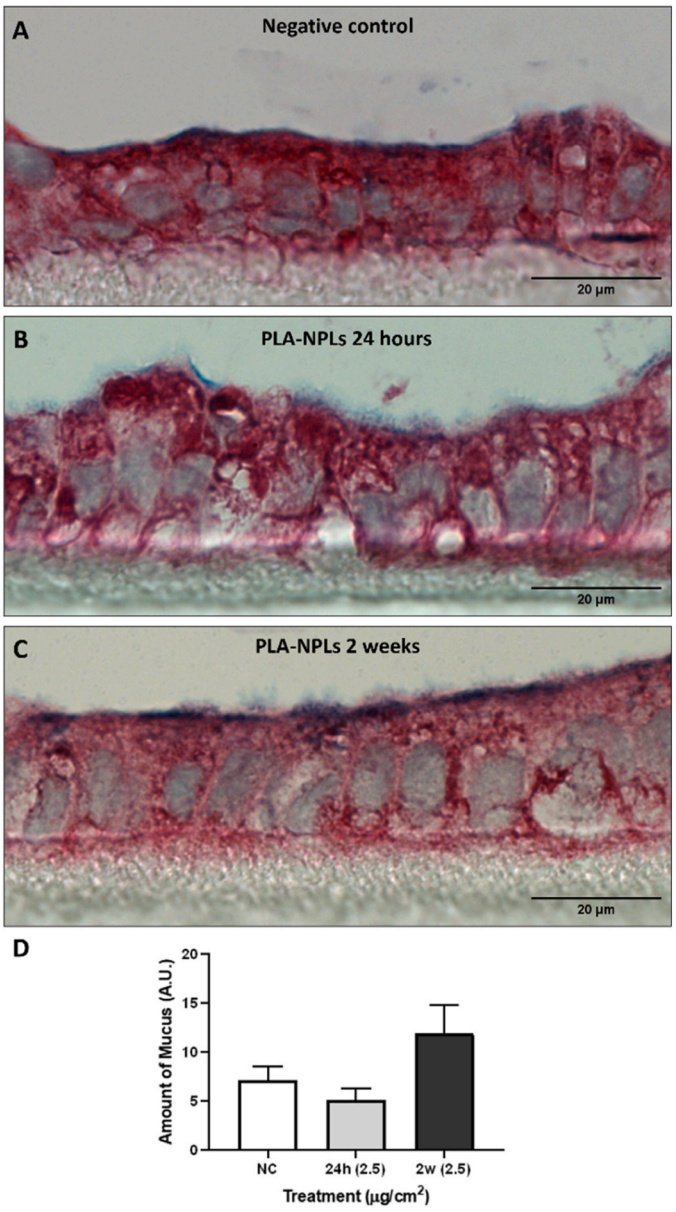

Fig. 7. Effects of PLA-NPLs on the mucus content of Calu-3 barrier. (A-C) Inverted light microscopy images of Calu-3 barriers stained with Alcian blue (mucus in blue) and hematoxylin and eosin stain (nuclei in purple-grey-ish and cell cytoplasm in pink). Thus, untreated (negative control), 24 h and 2 weeks exposed Calu-3 barriers to 2.5 µg/cm^2 PLA-NPLs, were stained and imaged for the mucus content analysis. (D) Measurements of mucus secretion with ImageJ. Data is expressed as mean ± SEM and analyzed by the one-way ANOVA ($p > 0.05$).

increases in the levels of acidic muco-substances were observed after exposures to TiO_2-NPs, alone or in combination with bacteria (*E. coli* and *L. rhamnosus)* [39]. The induction of mucus over-expression is a characteristic of numerous respiratory and inflammatory disease statuses like asthma and obstructive pulmonary disease, among others. Moreover, many cytokine and growth factor signaling pathways have been shown to trigger MUC5AC (a polymeric glycoproteins being one of the primary solid components of a mucus layer) expression (Symmes et al., 2021).

3.4. Genotoxic effects of PLA-NPLs by the comet assay

Genotoxicity has become an important endpoint to be considered in the Nanotoxicology field since shreds of evidence, such as high cell internalization and the presence of MNPLs into/close the cell nucleus, may result in serious consequences/effects translated into DNA damage. Good examples of that are metal-oxide nanoparticles, like TiO_2- and Ag-NPs, which are easily internalized by cells and rapidly transported to the cell nucleus causing severe DNA damage [21–23]. It should be stated that among the different biomarkers useful to determine human health risk, those detecting genotoxicity stand out. This is because, due to the relevant role of DNA in cell functionality, those structural and functional DNA lesions drastically compromise human health [11]. Therefore, in official regulations, genotoxicity is considered a surrogate biomarker of carcinogenesis [55].

In this study, we assessed both the general genotoxic damage (direct breaks in the DNA molecule) and the specific oxidative DNA damage (ODD) that occurs when the reactive oxygen species (ROS) interact with the DNA molecule, leading to modifications of DNA bases and the disruption of the DNA structure [23]. Increments in ODD can also be useful as an indirect way to measure intracellular ROS production. To such end, the comet assay -also known as single-cell gel electrophoresis assay- with and without the FPG (formamidopyrimidine DNA glycosylase) enzyme was used. Fig. 8 shows significant increments (compared to the negative control) in the levels of DNA damage, detected in all conditions, ranging from 4.54 % (24 h) and 5.33 % (1 w) to 7.01 % (2 w) (Fig. 8A). Interestingly, long-term exposures (2 weeks) to PLA-NPLs significantly increased the genotoxicity levels, compared to acute exposures (2.5 % increment). On the contrary, oxidative DNA damage induction was not detected in any of the PLA-NPLs treatments (Fig. 8B). This might indicate that the general DNA damage detected would be triggered by another mechanism different from the production of intracellular ROS (iROS), possibly by direct physical interaction with DNA strands, or with the replication machinery, as alternative mechanisms [32,51]. The amount of iROS was also checked by the DHE assay, but no significant inductions were detected as shown in (Fig. S1), reinforcing the previous ODD results. Similar results were observed when the *in vitro* barrier of Caco-2/HT29 cells was exposed to 50 and 100 µg/mL PLA-NPLs for 48 h, where no iROS induction was detected [6]. Contrarily, PS-COOH nanobeads were able to induce significant oxidative stress in Calu-3 barriers, associated with GSH depletion (measured by the monochlorobimane assay) [44]. In general, the induction of iROS levels has been observed to differ between cell types, exposure regimes, and the chemical nature of the polymer. Our previous investigations revealed that human primary cells, like HNEpCs, are sensitive tools for proper iROS detection when exposed to several types of polymers like polystyrene and polyethylene terephthalate [4]. Results on iROS detection, after exposing tumor-derived and/or immortalized cell lines (*e.g.*, Raji-B, THP-1, TK6, Caco-2, HT29, *etc.*) to different MNPLs, were controversial since unclear results were reported [18,53,57]. Using *in vivo* models, significant increases in the production of iROS, as well as oxidative DNA damage, were observed upon exposure to PLA-MNPLs [1,35,38,67].

In general, PLA and PLGA toxicity and genotoxicity studies have mainly focused on the biomechanical, optical, and biodegradable properties of the polymer for its use in clinical therapy as a biocompatible vehicle for drug transport (Helal-Neto et al., 2019). For example, membranes of PLA were developed as an alternative for medical devices and tested in CHO-K1 cells. The authors did not find any cytotoxic or genotoxic damage, as measured by the comet and micronucleus assays [60]. On the contrary, in human bronchial epithelial (16HBE14o-) cells PLGA-NPs (80 nm) with a positive surface charge induced chromosomal aberrations, as assessed by the micronucleus assay, at all tested concentrations (50 to 500 µg/mL). Nevertheless, no primary DNA damage was induced, as assessed by the comet assay (Platel et al., 2015). In another study, high concentrations of PLGA microspheres (0.4, 2, and 6 mg/mL) induced a significant elevation of the general DNA damage levels in both HUVECs and MSCs cells, after exposures lasting for 4 and 7 days [24,25,27,3,34,45,71,9]. Similarly, in *D. melanogaster* larvae

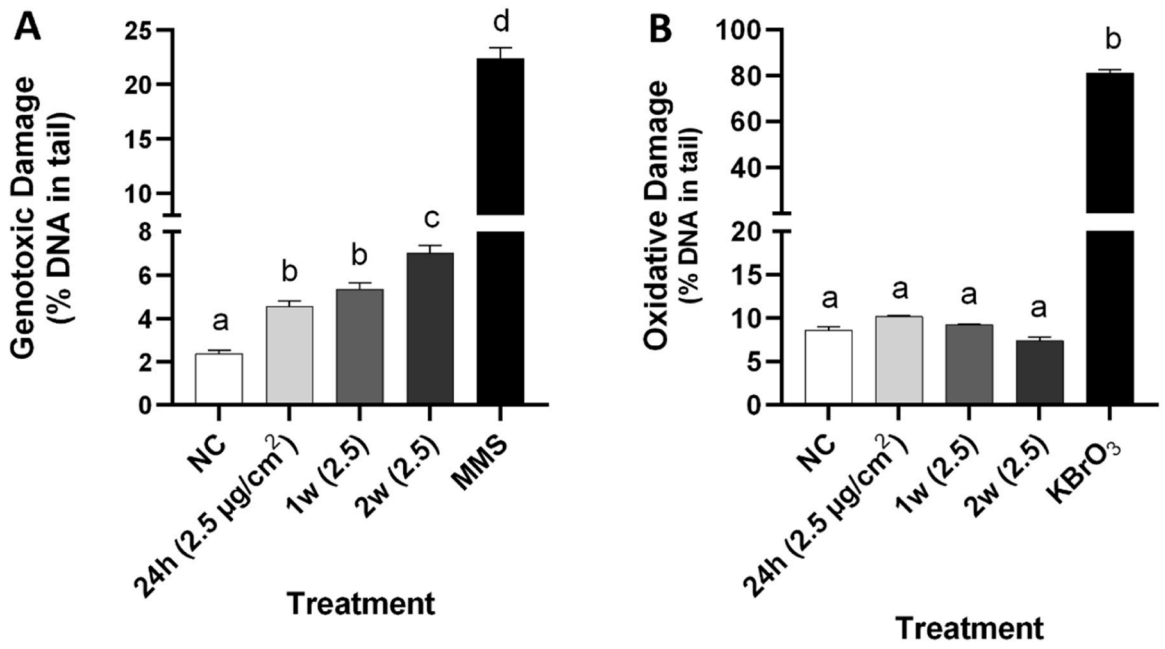

Fig. 8. Genotoxicity studies by using the comet assay. (A) General genotoxic damage of Calu-3 barriers after exposure to 0 (NC) and 2.5 μg/cm^2 for 24 h, 1, and 2 weeks. (B) Oxidative DNA damage of Calu-3 barriers after exposure to 0 (NC) and 2.5 μg/cm^2 for 24 h, 1, and 2 weeks. The positive controls used for genotoxic and oxidative damage were 200 μM MMS and 5 mM $KBrO_3$, respectively. Data is represented as mean ± SEM and analyzed using one-way ANOVA multiple comparisons with Dunnett's post-test. All those bars that do not share any letter are significantly different at $p \leq 0.05$.

exposed to PLA-NPLs (62.5, 250, and 1000 μg/g food) for all larval stages (up to 5 days) significant levels of DNA damage were induced [1,46,56,59,72]. Altogether, these results suggest that chronic and repeated exposures to biopolymers like PLA- and PLGA-NPLs might trigger DNA damage although the mechanisms of actions are not well understood yet. Due to the relevance of the obtained data, further investigations testing other *in vitro* and *in vivo* models, using complementary assays, and even testing other PLA-NPL forms, would be necessary to confirm the genotoxicity of PLA-NPLs and the involved mechanisms of action.

3.5. Secretome array analysis. Immune response of Calu-3 barriers

Being the frontline between the host and the environment, the bronchial epithelium is highly exposed to exogenous substances that highly stimulate innate immune responses and induce tissue damage. Accordingly, the previously observed alterations in tight junction expression and mucus content upon Calu-3 exposure to PLA-NPLs can be indicative of tissue damage induction (Figs. 3 and 4). A constant cycle of injury and abnormal repair of the epithelium can trigger chronic airway inflammation and remodeling [29]. Thus, a mechanistic understanding of injury susceptibility and damage responses, as well as the discovery of endpoints of effect, may lead to a more precise risk assessment of PLA-NPL exposure. To this end, we aimed to monitor the secretome of Calu-3 barriers after short- and long-term exposure to PLA-NPLs, by using the Human XL Cytokine Array Kit, as a rapid, sensitive, and economic tool to simultaneously detect cytokine expression differences between treatments. Accordingly, the relative expression levels of 105 soluble human proteins were determined and plotted, as indicated in Fig. 9, where only those showing the most statistical significance are represented. It is worth mentioning that the results of Calu-3 cells exposed to 1 and 2 weeks have been plotted in two distinct graphs for better separation and visualization of the columns and error bars (Fig. 9B and C). At first sight, longer and repeated exposures to PLA-NPLs trigger a more dramatic alteration of the epithelium secretome, since around 20 proteins were mostly over-expressed after 1 and 2 weeks of exposure, whilst only 5 proteins were detected to be up- or down-regulated after exposures lasting for 24 h. In addition, Fig. 10B shows a Venn diagram classifying the significantly secreted proteins for each type of treatment, highlighting the shared ones.

Among the altered proteins after exposures lasting for 24 h, CST3 and CCL20 were over-expressed, which are strong chemotactic cytokines for lymphocytes and neutrophils inducing a proinflammatory state of the bronchial epithelium. On the other hand, BSG, GDF-15, and PLAUR were under-expressed. These last proteins are related to different physiological pathways like (i) cell adhesion and migration, (ii) cell repair, and (iii) inflammation, respectively, which indicates that the *in vitro* bronchial epithelium is altered at different levels (See supplementary material for cytokine classification according to their function, and the respective references). However, many more proteins were altered at longer exposures (1 and 2 weeks) to PLA-NPLs. After a systemic literature search (PubMed), they could be divided into three big groups including (i) chemotaxis response, (ii) pro-inflammatory response, and (iii) tissue damage/repair response (Fig. 9B and C). In the first group, chemokines like CST3, CXCL12, CXCL1, MIF, and SPP1 were found to be significantly up-regulated, which eventually would induce the chemotaxis and migration of several immune cells (*i.e.*, neutrophils, leukocytes, eosinophils, macrophages, *etc.*). Among those, it is worth highlighting the activity of CXCL1 and MIF, which have been described with pro-inflammatory activity, leading to airway remodeling, and acting in acute lung injury and wound repair, respectively. Moreover, SPP1 is found at high levels in airway secretions (sputum and bronchoalveolar fluid) during chronic airway inflammation such as in patients with asthma, cystic fibrosis, and chronic obstructive pulmonary diseases (COPD) (see supplementary Table S1). In the second group, well-known cytokines like IL-17A, GC, DPP4, CRP, RETN, and ICAM-1 classified as pro-inflammatory cytokines and/or proteins related to an inflammatory response, and IL-1RN and CFD as anti-inflammatory activity, are present. From this group, CRP and GC are widely used as inflammatory markers, which can predict several diseases like cardiovascular disease and COPD, respectively (Table S1). Finally, in the third group, proteins related to the process of tissue damage repair, including several growth factors like TFF3, EGF, and FGF-19, related proteins like IGFBP-2 and − 3, and other proteins specifically involved in tissue

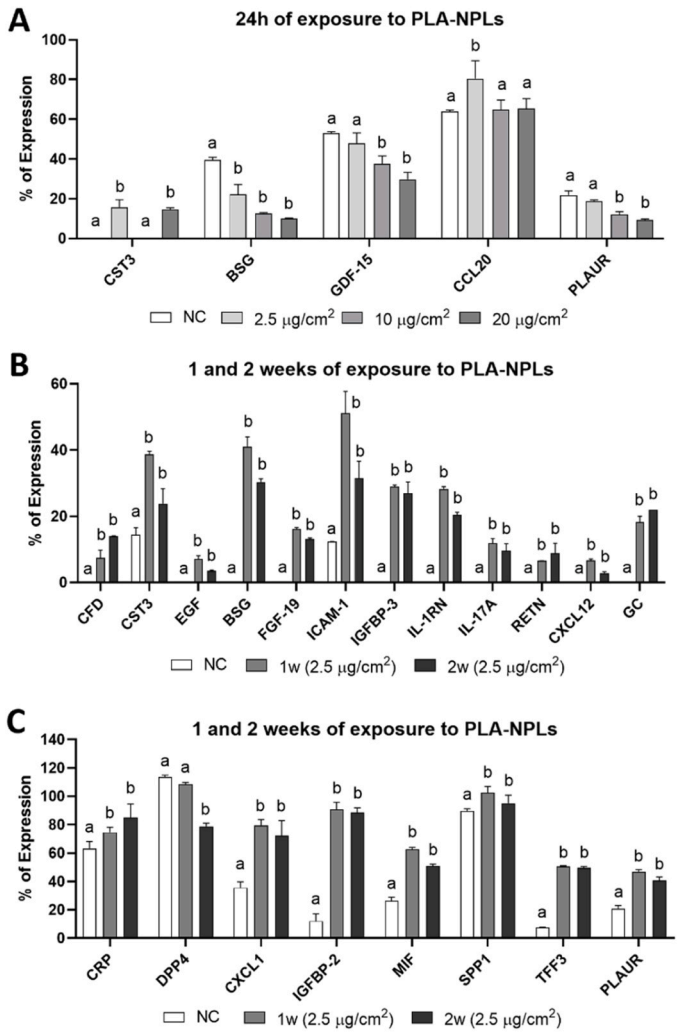

Fig. 9. Proteome array analysis. A proteome profiler array (The human XL cytokine array) was used to investigate the inflammatory response of the Calu-3 barriers upon PLA-NPL exposures. (A) Calu-3 barriers exposed to 0 (NC), 2.5, 10, and 20 μg/cm^2 of PLA-NPLs for 24 h. (B and C) Calu-3 barriers were exposed to 0 and 2.5 μg/cm^2 of PLA-NPLs for 1 and 2 weeks, respectively. Data is represented as mean ± SEM and analyzed using the one-way ANOVA with Dunnett's post-test. All those bars that do not share any letter are significantly different at $p \leq 0.05$. The lack of NC values, in several cases, is due to the absence of measurable expression for these cytokines. This is also applicable to the lack of other columns.

remodeling like PLAUR were also found up-regulated. Besides their involvement in lung pattern formation during organogenesis, growth factors can be implicated in modulating injury-repair responses of the adult lung. Similarly, TFF3 functions go from mucosa protection, by thickening the mucus, to increasing epithelial healing rates (Table S1).

A deeper analysis of the cytokine array results was completed using the STRING database (Fig. 10). Briefly, STRING is a bioinformatic resource providing information about protein-protein interactions (PPI), their biological classification, and/or significance. STRING integrates curated experimental data, as well as computationally predicted interactions from various sources, to provide functional enrichment diagrams. Hence, the functional enrichment network obtained from the analysis of those proteins significantly secreted, after the exposure to PLA-NPLs for 1 and 2 weeks, was (obviously) complex (Fig. 10A). The obtained PPI enrichment p-value was $\leq 1.0 \times 10^{-16}$ and the functional classification involved several biological processes like responses to chemicals and stress stimulus, as well as chemotaxis and inflammation.

From the literature search, significant differences in the cytokine pattern were observed when exposing whole blood samples (as an *ex vivo* model) to 10 and 25 μg/mL of PS-NPLs. Thus, while at the lowest concentration of PS-NPLs, most of the cytokines were under-expressed, the trend was completely inverted at higher concentrations, where cytokines like TGFα, IL31, CXCL10, IL1α, IL1β, IL3, IL15, IL34, and TNFα were found to be significantly up-regulated [5]. On the contrary, no significant increments of pro-inflammatory cytokines after the treatment of A549 cells to 2, 20, and 200 μg/mL PLA-NPLs for 24, 48, and 72 h were observed. Only IL-12P70, VEGF, and IL-15 were significantly under-expressed. However, when a proteomic evaluation (with 278 dysregulated polypeptides) was performed, several biological functions such as glycolysis, biosynthesis, stress response, and host-virus interaction were significantly compromised [16]. It is worth mentioning that, in comparison to da Luz and co-workers' study, we have used a more realistic *in vitro* environment of the bronchial epithelium and a more relevant exposure regime, since longer and repeated treatments were performed to simulate the continuous human inhalation of environmental pollutants. In this sense, the Calu-3 barrier model in ALI conditions has never been used to determine the harmful and long-term effects of MNPLs. In addition, we have used true-to-life PLA-NPLs (containing plastic additives), while the referred work used pristine engineered PLA-NPLs. Focusing on the effects of petroleum-based NPLs, significant changes in the cytokine production (IL-6 and 8) were observed after exposing A549 barriers to PS-NPLs (carboxilated 20 and 200 nm, pristine and aminated 200 nm-NPLs), but not when treating Calu-3 barriers [40]. Similarly, alterations in the expression of cytokines, using A549 cells and pristine PS-NPLs were reported, showing a significant up-regulation of pro-inflammatory cytokines such as IL-8, NF-κB, and TNF-α [68]. Interestingly, high expression levels of inflammatory cytokines, as well as in the levels of fibrosis-related factors, were observed in the lungs of ICR mice exposed to polystyrene NPLs [31].

4. Conclusions

The increasing use of bio-based polymers in several fields, including the food industry (for food packaging and single-use cutlery), biomedicine (to develop more biocompatible medical devices), and the pharmaceutic industry (for drug and chemical transport and delivery) has dramatically increased the human exposure to biopolymers so-called "biodegradable plastics". However, the "biodegradable" terminology can be controversial since there is multiple evidence demonstrating that under physiological conditions, bio-based plastics do not easily "disappear" [15]. Accordingly, the constant human exposure to MNPLs able to bio-persist and accumulate in several tissues and organs has called the attention of regulators, stakeholders, and scientists.

In this context, this study aimed to monitor the journey of degradation products (NPLs) from PLA plastics (as a model of a widely used bioplastic) and evaluate their potential detrimental effects on an *in vitro* model of the human bronchial epithelium (the Calu-3 barrier model), using a reliable exposure approach in air-liquid (ALI) interaction conditions. To such an end, we have monitored the PLA-NPLs internalization, their effect on the barrier structure (mucus content, TJ expression, TEER, and LY), the intracellular ROS production, the genotoxic effects, and the cytokine release, after short and long-term exposures. Our results indicated that exposures to PLA-NPLs might compromise the barrier stability since the expression of tight junctions was significantly decreased. In addition, the mucus secretion was increased after the long-term exposures to PLA-NPLs, although no statistical significance was reached. Already at 24 h, PLA-NPLs internalized a vast number of cells in a dose-dependent manner. PLA-NPLs interact physically with the cell nuclei, suggesting that PLA-NPLs might affect the proper DNA function and structure. Thus, the use of the comet assay confirmed the genotoxic effects of PLA-NPL exposure since the general DNA damage levels increased significantly at all the tested exposure regimes. On the contrary, no iROS nor oxidative DNA damage induction was observed. Finally, and as a valuable approach, long-term exposures to PLA-NPLs

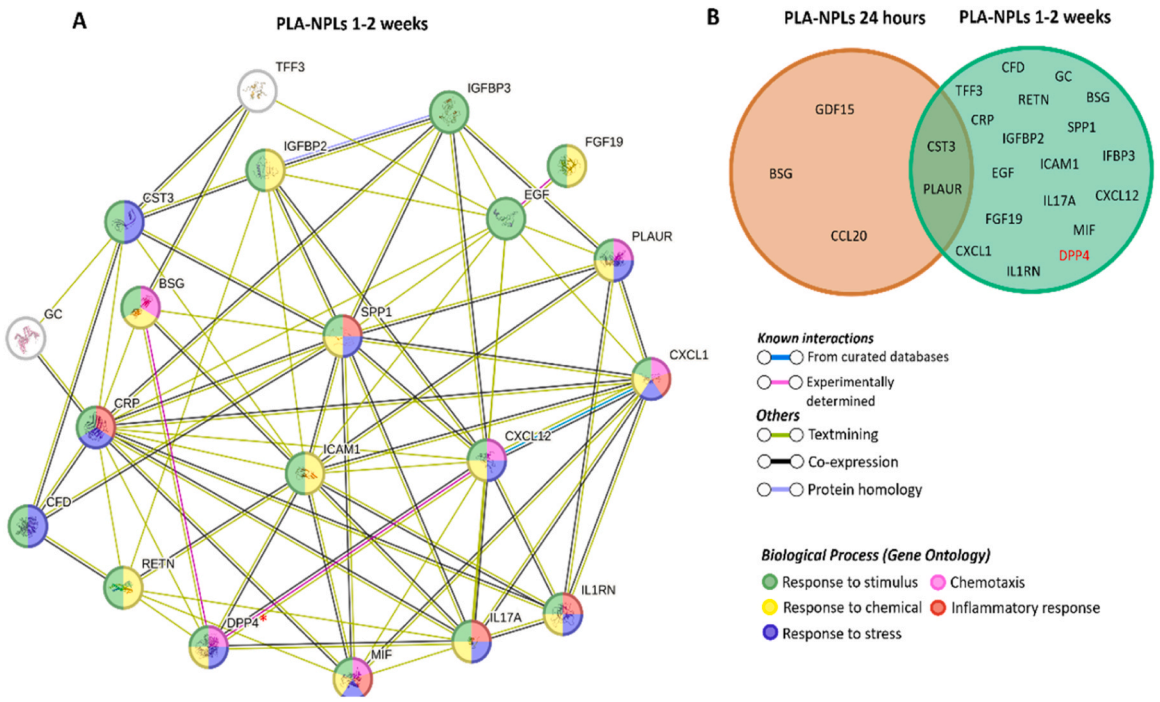

Fig. 10. STRING analysis. (A) Functional cytokines association network of the significantly altered cytokines after exposing the *in vitro* Calu-3 barrier to 2.5 μg/cm^2 PLA-NPLs for 1 and 2 weeks. The color of the nodules represents the functions or biological processes in which they are involved. (B) Venn diagram showing the significantly altered proteins after short- (24 h) and long-term (1 and 2 weeks) exposures to 2.5 μg/cm^2 PLA-NPLs. Proteins highlighted in red are significantly under-expressed.

significantly up-regulated the secretion of multiple proteins and cytokines related to tissue damage and remodeling, chemotaxis, pro-inflammatory response, and response to chemicals and stress stimulus.

In general terms, we have found that (i) the *in vitro* model Calu-3 barrier is a suitable system for relatively long-term and repeated exposures, compared to other *in vitro* cell culture-based models; (ii) long-term exposures to PLA-NPLs might be inducing exacerbating epithelial damage and remodeling or injury-repair signal when compared to acute exposures; (iii) PLA-NPLs presents significant genotoxic activity but not oxidative effects since the particles rapidly translocate to the nuclear compartment of the epithelial cells and physically interacting with the DNA, and (iv) the Human XL cytokine array has shown to be a rapid and high-throughput tool for studying endpoint of effects and for potential biomarker discovery. Equally important to the previous conclusions, this study unravels the intricacies of the imposed "eco-friendly" paradigm surrounding biodegradable and biocompatible polymers by further understanding their mechanisms of action on human health.

Environmental implication

Environmental micro/nanoplastics (MNPLs), as emergent pollutants, are of special environmental/health concern, and determining their potential risk is an urgent requirement. In this context, special attention must be paid to bio-based polymers at the nano-size (nanoplastics; NPLs), which have been demonstrated to rapidly cross human barriers, internalize cells, and interact at the molecular level. These bio-based polymers, in opposition to petroleum-based polymers, are gaining popularity (as used in many consumer products) increasing their environmental presence as a plastic waste. Consequently, further efforts are required to determine their potentially harmful effects. From this point of view, and as a novelty, our study apport data on the interaction and effects of polylactic acid (PLA)-NPLs (a widely use bioplastic) with an in vitro model of the human bronchial epithelium barrier. Due to the increasing relevance of MNPLs as airborne pollutants our results contribute to a better understanding of the risk associated with this exposure route.

CRediT authorship contribution statement

Iris Romero-Andrada: Investigation. **Alicia Lacoma:** Investigation. **Aliro Villacorta:** Investigation, Data curation. **Jessica Arribas Arranz:** Validation, Investigation. **Javier Gutiérrez:** Methodology, Investigation, Data curation. **Alba Garcia-Rodriguez:** Writing – original draft, Supervision, Data curation, Conceptualization. **Laura Rubio:** Writing – original draft, Supervision, Investigation. **Ricard Marcos:** Writing – review & editing, Conceptualization. **Alba Hernández:** Writing – review & editing, Supervision, Conceptualization.

Declaration of Competing Interest

The authors declare that they have no known competing financial interests or personal relationships that could have appeared to influence the work reported in this paper.

Data availability

Data will be made available on request.

Acknowledgments

J. Gutiérrez holds a PIF Ph.D. fellowship from the Universitat Autònoma de Barcelona. A. Villacorta was supported by a Ph.D. fellowship from the National Agency for Research and Development (ANID), CONICYT PFCHA / DOCTORADO BECAS CHILE / 2020−72210237. A. García-Rodríguez received funding from the post-doctoral fellowship program Beatriu de Pinós, funded by the Secretary of Universities and Research [Government of Catalonia] and by the Horizon 2020 program of Research and Innovation of the European Union under the Marie Sklodowska-Curie grant agreement No 801370. L. Rubio holds a postdoctoral Juan de la Cierva contract (IJC2020-2686I/

AEI/10.13039/501100011033). A. Hernández was granted an ICREA ACADEMIA award.

This project (PlasticHeal) has received funding from the European Union's Horizon 2020 research and innovation programme under grant agreement No 965196. This work was partially supported by the Spanish Ministry of Science and Innovation [PID2020-116789, RB-C43], and the Generalitat de Catalunya (2021-SGR-00731).

Appendix A. Supporting information

Supplementary data associated with this article can be found in the online version at doi:10.1016/j.jhazmat.2024.134900.

References

[1] Alaraby, M., Abass, D., Hernández, A., Marcos, R., 2024. Are bioplastics safe? Hazardous effects of polylactic acid (PLA) nanoplastics in *Drosophila*, 2024 Sci Total Environ 919 (2), 170592. https://doi.org/10.1016/j.scitotenv.2024.170592.

[2] Allen, D., Allen, S., Abbasi, S., et al., 2022. Microplastics and nanoplastics in the marine-atmosphere environment. Nat Rev Earth Environ 3, 393–405. Doi: 10.1038/s43017-022-00292-x.

[3] Annangi, B., Villacorta, A., López-Mesas, M., Fuentes-Cebrian, V., Marcos, R., Hernández, S., 2023. Hazard assessment of polystyrene nanoplastics in primary human nasal epithelial cells, focusing on the autophagic effects. Biomolecules 13 (2023), 220. https://doi.org/10.3390/biom13020220.

[4] Annangi, B., Villacorta, A., Vela, L., Tavakolpournegari, A., Marcos, R., Hernández, A., 2023. Effects of true-to-life PET nanoplastics using primary human nasal epithelial cells. Environ Toxicol Pharmacol 100, 104140. https://doi.org/10.1016/j.etap.2023.104140.

[5] Ballesteros, S., Domenech, J., Barguilla, I., Cortés, C., Marcos, R., Hernández, A., 2020. Genotoxic and immunomodulatory effects in human white blood cells after *ex vivo* exposure to polystyrene nanoplastics. Environ Sci: Nano 7, 3431–3446. https://doi.org/10.1039/D0EN00748J.

[6] Banaei, G., García-Rodríguez, A., Tavakolpournegari, A., Martín-Pérez, A., Villacorta, A., Marcos, R., et al., 2023. The release of polylactic acid nanoplastics (PLA-NPLs) from commercial teabags. Obtention, characterization, and hazard effects of true-to-life PLA-NPLs. J Hazard Mater 458, 131899. https://doi.org/10.1016/j.jhazmat.2023.131899.

[7] Bayarri, M.A., Milara, J., Estornut, C., Cortijo, J., 2021. Nitric oxide system and bronchial epithelium: more than a barrier. Front Physiol 12, 687381. https://doi.org/10.3389/fphys.2021.687381.

[8] Bergmann, M., Collard, F., Fabres, J., Gabrielsen, G.W., Provencher, J.F., Rochman, C.M., et al., 2022. Plastic pollution in the Arctic. Nat Rev Earth Environ 3, 323–337. https://doi.org/10.1038/s43017-022-00279-8.

[9] Brouwer, H., Porbahaie, M., Boeren, S., Busch, M., Bouwmeester, H., 2024. The *in vitro* gastrointestinal digestion-associated protein corona of polystyrene nano- and microplastics increases their uptake by human THP-1-derived macrophages. Part Fibre Toxicol 21 (1), 4. https://doi.org/10.1186/s12989-024-00563-z.

[10] Busch, M., Brouwer, H., Aalderink, G., Bredeck, G., Kämpfer, A.A.M., Schins, R.P. F., et al., 2023. Investigating nanoplastics toxicity using advanced stem cell-based intestinal and lung *in vitro* models. Front Toxicol 5, 1112212. https://doi.org/10.3389/ftox.2023.1112212.

[11] Carbone, M., Arron, S.T., Beutler, B., Bononi, A., Cavenee, W., Cleaver, J.E., et al., 2020. Tumour predisposition and cancer syndromes as models to study gene-environment interactions. Nat Rev Cancer 20 (9), 533–549 doi: 10.1038/ s41568-020-0265-y.

[12] Catarino, A.I., Macchia, V., Sanderson, W.G., Thompson, R.C., Henry, T.B., 2018. Low levels of microplastics (MP) in wild mussels indicate that MP ingestion by humans is minimal compared to exposure via household fibres fallout during a meal. Environ Pollut 237, 675–684. https://doi.org/10.1016/j.envpol.2018.02.069.

[13] Chen, H., 2022. Biodegradable plastics in the marine environment: a potential source of risk. Water Emerg Contam Nanoplastics 1, 16. https://doi.org/10.20517/wecn.2022.11.

[14] Chivé, C., Mc Cord, C., Sanchez-Guzman, D., Brookes, O., Joseph, P., Lai Kuen, R., et al., 2023. 3D model of the bronchial epithelial barrier to study repeated exposure to xenobiotics: application to silver nanoparticles. Environ Toxicol Pharmacol 103, 104281. https://doi.org/10.1016/j.etap.2023.104281.

[15] Colwell, J., Pratt, S., Lant, P., Laycock, B., 2023. Hazardous state lifetimes of biodegradable plastics in natural environments. Sci Total Environ 894, 165025. https://doi.org/10.1016/j.scitotenv.2023.165025.

[16] da Luz, C.M., Boyles, M.S., Falagan-Lotsch, P., Pereira, M.R., Tutumi, H.R., de Oliveira Santos, E., et al., 2017. Polylactic acid nanoparticles (PLA-NP) promote physiological modifications in lung epithelial cells and are internalized by clathrin-coated pits and lipid rafts. J Nanobiotechnol 15, 11. https://doi.org/10.1186/s12951-016-0238-1.

[17] Deng, Y., Yang, P., Tan, H., Shen, R., Chen, D., 2023. Polylactic acid microplastics do not exhibit lower biological toxicity in growing mice compared to polyvinyl chloride microplastics. J Agric Food Chem 71 (49), 19772–19782. https://doi.org/10.1021/acs.jafc.3c06576.

[18] Domenech, J., Hernández, A., Rubio, L., Marcos, R., Cortés, C., 2020. Interactions of polystyrene nanoplastics with *in vitro* models of the human intestinal barrier. Arch Toxicol 94 (9), 2997–3012. https://doi.org/10.1007/s00204-020-02805-3.

[19] Elje, E., Mariussen, E., McFadden, E., Dusinska, M., Rundén-Pran, E., 2023. Different sensitivity of advanced bronchial and alveolar mono- and coculture models for hazard assessment of nanomaterials. Nanomaterials 13 (3), 407. https://doi.org/10.3390/nano13030407.

[20] Filipe, V., Hawe, A., Jiskoot, W., 2010. Critical evaluation of nanoparticle tracking analysis (NTA) by NanoSight for the measurement of nanoparticles and protein aggregates. Pharm Res 27 (5), 796–810. https://doi.org/10.1007/s11095-010-0073-2.

[21] García-Rodríguez, A., Vila, L., Cortés, C., Hernández, A., Marcos, R., 2018. Effects of differently shaped TiO_2NPs (nanospheres, nanorods and nanowires) on the *in vitro* model (Caco-2/HT29) of the intestinal barrier. Part Fibre Toxicol 15 (1), 33. https://doi.org/10.1186/s12989-018-0269-x.

[22] García-Rodríguez, A., Kazantseva, L., Vila, L., Rubio, L., Velázquez, A., Ramírez, M. J., et al., 2019. Micronuclei detection by flow cytometry as a high-throughput approach for the genotoxicity testing of nanomaterials. Nanomater (Basel) 9 (12), 1677. https://doi.org/10.3390/nano9121677.

[23] García-Rodríguez, A., Rubio, L., Vila, L., Xamena, N., Velázquez, A., Marcos, R., et al., 2019. The comet assay as a tool to detect the genotoxic potential of nanomaterials. Nanomaterials 9 (10), 1385. https://doi.org/10.3390/nano9101385.

[24] García-Rodríguez, A., Stillwell, A., Tochilovsky, B., Tanzman, J.V., Limage, R., Kolba, N., et al., 2022. The mechanistic effects of human digestion on magnesium oxide nanoparticles: implications for probiotics *Lacticaseibacillus rhamnosus* GG and *Bifidobacterium bifidum* VPI 1124. Environ Sci Nano 9 (12), 4540–4557. https://doi.org/10.1039/d2en00150k.

[25] Gon, Y., Hashimoto, S., 2022. Role of airway epithelial barrier dysfunction in pathogenesis of asthma. Allergol Int 67 (1), 12–17. https://doi.org/10.1016/j.alit.2017.08.011.

[26] He, R.W., Braakhuis, H.M., Vandebriel, R.J., Staal, Y.C.M., Gremmer, E.R., Fokkens, P.H.B., et al., 2021. Optimization of an air-liquid interface *in vitro* cell co-culture model to estimate the hazard of aerosol exposures. J Aerosol Sci 153, 105703. https://doi.org/10.1016/j.jaerosci.2020.105703.

[27] Helal-Neto, E., de Barros, A.Od.S., Saldanha-Gama, R., Brandão-Costa, R., Alencar, L.M.R., dos Santos, C.C., et al., 2020. Molecular and cellular risk assessment of healthy human cells and cancer human cells exposed to nanoparticles. Int J Mol Sci 21 (1), 230. https://doi.org/10.3390/ijms21010230.

[28] Hill, D.B., Button, B., Rubinstein, M., Boucher, R.C., 2022. Physiology and pathophysiology of human airway mucus. Physiol Rev 102 (4), 1757–1836. https://doi.org/10.1152/physrev.00004.2021.

[29] Jakiela, B., Rebane, A., Soja, J., Bazan-Socha, S., Laanesoo, A., Plutecka, H., et al., 2021. Remodeling of bronchial epithelium caused by asthmatic inflammation affects its response to rhinovirus infection. Sci, Rep 11 (1), 12821. https://doi.org/10.1038/s41598-021-92252-6.

[30] Jenner, L.C., Rotchell, J.M., Bennett, R.T., Cowen, M., Tentzeris, V., Sadofsky, L.R., 2022. Detection of microplastics in human lung tissue using μFTIR spectroscopy. Sci Total Environ 831, 154907. https://doi.org/10.1016/j.scitotenv.2022.154907.

[31] Jin, Y.J., Kim, J.E., Roh, Y.J., Song, H.J., Seol, A., Park, J., et al., 2023. Characterisation of changes in global genes expression in the lung of ICR mice in response to the inflammation and fibrosis induced by polystyrene nanoplastics inhalation. Toxicol Res 39 (4), 1–25. https://doi.org/10.1007/s43188-023-00188-y.

[32] Joksimovic, N., Selakovic, D., Jovicic, N., Jankovic, N., Pradeepkumar, P., Eftekhari, A., et al., 2022. Nanoplastics as an invisible threat to humans and the environment. J Nanomater 2022, 6707819. https://doi.org/10.1155/2022/6707819.

[33] Karkri, M., 2017. Thermal conductivity of biocomposite materials. In: Sadasivuni, K.K., Ponnamma, D., Kim, J., Cabibihan, J.-J., AlMaadeed, M.A. (Eds.), In: Biopolymer Composites in Electronics. Elsevier, pp. 129–153. https://doi.org/10.1016/B978-0-12-809261-3.00004-8.

[34] Kessler, A., Hedberg, J., Blomberg, E., Odnevall, I., 2022. Reactive oxygen species formed by metal and metal oxide nanoparticles in physiological media -a review of reactions of importance to nanotoxicity and proposal for categorization. Nanomaterials 12 (11), 1922. https://doi.org/10.3390/nano12111922.

[35] Khosrovyan, A., Melkonyan, H., Rshtuni, L., Gabrielyan, B., Kahru, A., 2023. Polylactic acid-based microplastic particles induced oxidative damage in brain and gills of goldfish *Carassius auratus*. Water 15, 2133. https://doi.org/10.3390/w15112133.

[36] Kim, K.H., Kabir, E., Kabir, S., 2015. A review on the human health impact of airborne particulate matter. Environ Int 74, 136–143. https://doi.org/10.1016/j.envint.2014.10.005.

[37] Kumari, S., Rao, A., Kaur, M., Dhania, G., 2023. Petroleum-based plastics versus bio-based plastics: a review. Nat Environ Pollut Technol 22 (3), 1111–1124. https://doi.org/10.46488/NEPT.2023.v22i03.003.

[38] Legaz, S., Exposito, J.Y., Lethias, C., Viginier, B., Terzian, C., Verrier, B., 2016. Evaluation of polylactic acid nanoparticles safety using *Drosophila* model. Nanotoxicology 10 (8), 1136–1143. https://doi.org/10.1080/17435390.2016.1181806.

[39] Limage, R., Tako, E., Kolba, N., Guo, Z., García-Rodríguez, A., Marques, C.N.H., et al., 2020. TiO_2 nanoparticles and commensal bacteria alter mucus layer thickness and composition in a gastrointestinal tract model. Small 16 (21), e2000601. https://doi.org/10.1002/smll.202000601.

[40] Meindl, C., Öhlinger, K., Zrim, V., Steinkogler, T., Fröhlich, E., 2021. Screening for effects of inhaled nanoparticles in cell culture models for prolonged exposure. Nanomater (Basel) 11 (3), 606. https://doi.org/10.3390/nano11030606.
[41] Meziu, E., Shehu, K., Koch, M., Schneider, M., Kraegeloh, A., 2023. Impact of mucus modulation by *N*-acetylcysteine on nanoparticle toxicity. Int J Pharm X 6, 100212. https://doi.org/10.1016/j.ijpx.2023.100212.
[42] Mura, S., Hillaireau, H., Nicolas, J., Le Droumaguet, B., Gueutin, C., Zanna, S., et al., 2011. Influence of surface charge on the potential toxicity of PLGA nanoparticles towards Calu-3 cells. Int J Nanomed 6, 2591–2605. https://doi.org/10.2147/IJN.S24552.
[43] Mura, S., Hillaireau, H., Nicolas, J., Kerdine-Römer, S., Le Droumaguet, B., Deloménie, C., et al., 2011. Biodegradable nanoparticles meet the bronchial airway barrier: how surface properties affect their interaction with mucus and epithelial cells. Biomacromolecules 12 (11), 4136–4143. https://doi.org/10.1021/bm201226x.
[44] Paget, V., Dekali, S., Kortulewski, T., Grall, R., Gamez, C., Blazy, K., et al., 2015. Specific uptake and genotoxicity induced by polystyrene nanobeads with distinct surface chemistry on human lung epithelial cells and macrophages. PLoS One 10 (4), e0123297. https://doi.org/10.1371/journal.pone.0123297.
[45] PATROLS, 2022. PATROLS SOP Handbook. 2021. Available from: ⟨https://patrols-h2020.eu/publications/sops/index.php⟩.
[46] Platel, A., Carpentier, R., Becart, E., Mordacq, G., Betbeder, D., Nesslany, F., 2016. Influence of the surface charge of PLGA nanoparticles on their *in vitro* genotoxicity, cytotoxicity, ROS production and endocytosis. J Appl Toxicol 36 (3), 434–444. https://doi.org/10.1002/jat.3247.
[47] Prata, J.C., 2018. Airborne microplastics: consequences to human health. Environ Pollut 234, 115–126. https://doi.org/10.1016/j.envpol.2017.11.043.
[48] Prata, J.C., da Costa, J.P., Lopes, I., Duarte, A.C., Rocha-Santos, T., 2020. Environmental exposure to microplastics: An overview on possible human health effects. Sci Total Environ 702, 134455. https://doi.org/10.1016/j.scitotenv.2019.134455.
[49] Revel, M., Châtel, A., Mouneyrac, C., 2018. Micro(nano) plastics: a threat to human health? Curr Opin Environ Sci Health 1, 17–23. https://doi.org/10.1016/j.coesh.2017.10.003.
[50] Rosli, N.A., Karamanlioglu, M., Kargarzadeh, H., Ahmad, I., 2021. Comprehensive exploration of natural degradation of poly(lactic acid) blends in various degradation media: a review. Int J Biol Macromol 187, 732–741. https://doi.org/10.1016/j.ijbiomac.2021.07.
[51] Roursgaard, M., Hezareh Rothmann, M., Schulte, J., Karadimou, I., Marinelli, E., Møller, P., 2022. Genotoxicity of particles from grinded plastic items in Caco-2 and HepG2 cells. Front Pub Health 10, 906430. https://doi.org/10.3389/fpubh.2022.906430.
[52] Rubio, L., Marcos, R., Hernández, A., 2020. Potential adverse health effects of ingested micro- and nanoplastics on humans. Lessons learned from *in vivo* and *in vitro* mammalian models. J Toxicol Environ Health B Crit Rev 23 (2), 51–68. https://doi.org/10.1080/10937404.2019.1700598.
[53] Rubio, L., Barguilla, I., Domenech, J., Marcos, R., Hernández, A., 2020. Biological effects, including oxidative stress and genotoxic damage, of polystyrene nanoparticles in different human hematopoietic cell lines. J Hazard Mater 398, 122900. https://doi.org/10.1016/j.jhazmat.2020.122900.
[54] Setyawati, M.I., Tay, C.Y., Bay, B.H., Leong, D.T., 2017. Gold nanoparticles induced endothelial leakiness depends on particle size and endothelial cell origin. ACS Nano 11 (5), 5020–5030. https://doi.org/10.1021/acsnano.7b01744.
[55] Shi, X., Wang, X., Huang, R., Tang, C., Hu, C., Ning, P., et al., 2022. Cytotoxicity and genotoxicity of polystyrene micro- and nanoplastics with different size and surface modification in A549 cells. Int J Nanomed 17, 4509–4523. https://doi.org/10.2147/IJN.S381776.
[56] Symmes, B.A., Stefanski, A.L., Magin, C.M., Evans, C.M., 2018. Role of mucins in lung homeostasis: regulated expression and biosynthesis in health and disease. Biochem Soc Trans 46 (3), 707–719. https://doi.org/10.1042/BST20170455.
[57] Tavakolpournegari, A., Annangi, B., Villacorta, A., Banaei, G., Martin, J., Pastor, S., et al., 2023. Hazard assessment of different-sized polystyrene nanoplastics in hematopoietic human cell lines. Chemosphere 325, 138360. https://doi.org/10.1016/j.chemosphere.2023.138360.
[58] Tsuji, H., Ikarashi, K., 2004. *In vitro* hydrolysis of poly(l-lactide) crystalline residues as extended-chain crystallites. Part I: long-term hydrolysis in phosphate-buffered solution at 37°C. Biomaterials 25 (24), 5449–5455. https://doi.org/10.1016/j.biomaterials.2003.12.053.
[59] UNDESA. 2015. Global Sustainable Development Report https://sustainabledevelopment.un.org/content/documents/1758GSDR%202015%20Advance%20Unedited%20Version.pdf.
[60] Uzun, N., Martins, T.D., Teixeira, G.M., Cunha, N.L., Oliveira, R.B., Nassar, E.J., et al., 2015. Poly(L-lactic acid) membranes: absence of genotoxic hazard and potential for drug delivery. Toxicol Lett 232 (2), 513–518. https://doi.org/10.1016/j.toxlet.2014.11.032.
[61] Van Den Broucke, S., Vanoirbeek, J.A.J., Derua, R., Hoet, P.H.M., Ghosh, M., 2021. Effect of graphene and graphene oxide on airway barrier and differential phosphorylation of proteins in tight and adherents junction pathways. Nanomater (Basel) 11 (5), 1283. https://doi.org/10.3390/nano11051283.
[62] Vela, L., Villacorta, A., Venus, T., Estrela-Lopis, I., Pastor, S., García-Rodriguez, A., et al., 2023. The potential effects of *in vitro* digestion on the physicochemical and biological characteristics of polystyrene nanoplastics. Environ Pollut 329, 121656. https://doi.org/10.1016/j.envpol.2023.121656.
[63] Vethaak, A.D., Legler, J., 2021. Microplastics and human health. Science 371 (6530), 672–674. https://doi.org/10.1126/science.abe5041.
[64] Villacorta, A., Rubio, L., Alaraby, M., López-Mesas, M., Fuentes-Cebrian, V., Moriones, O.H., et al., 2022. A new source of representative secondary PET nanoplastics. Obtention, characterization, and hazard evaluation. J Hazard Mater 439, 129593. https://doi.org/10.1016/j.jhazmat.2022.129593.
[65] Wang, M., Li, Q., Shi, C., Lv, J., Xu, Y., Yang, J., et al., 2023. Oligomer nanoparticle release from polylactic acid plastics catalysed by gut enzymes triggers acute inflammation. Nat Nanotechnol 18 (4), 403–411. https://doi.org/10.1038/s41565-023-01329-y.
[66] Water, J.J., Smart, S., Franzyk, H., Foged, C., Nielsen, H.M., 2015. Nanoparticle-mediated delivery of the antimicrobial peptide plectasin against *Staphylococcus aureus* in infected epithelial cells. Eur J Pharm Biopharm 92, 65–73. https://doi.org/10.1016/j.ejpb.2015.02.009.
[67] Wiese-Rischke, C., Murkar, R.S., Walles, H., 2021. Biological models of the lower human airways-challenges and special requirements of human 3D barrier models for biomedical research. Pharmaceutics 13 (12), 2115. https://doi.org/10.3390/pharmaceutics13122115.
[68] Wu, X., Zhang, X., Chen, X., Ye, A., Cao, J., Hu, X., et al., 2023. The effects of polylactic acid bioplastic exposure on midgut microbiota and metabolite profiles in silkworm (*Bombyx mori*): an integrated multi-omics analysis. Environ Pollut 334, 122210. https://doi.org/10.1016/j.envpol.2023.122210.
[69] Xu, M., Halimu, G., Zhang, Q., Song, Y., Fu, X., Li, Y., et al., 2019. Internalization and toxicity: a preliminary study of effects of nanoplastic particles on human lung epithelial cell. Sci Total Environ 694, 133794. https://doi.org/10.1016/j.scitotenv.2019.133794.
[70] Yang, S., Cheng, Y., Chen, Z., Liu, T., Yin, L., Pu, Y., et al., 2021. *In vitro* evaluation of nanoplastics using human lung epithelial cells, microarray analysis and co-culture model. Ecotoxicol Environ Saf 226, 112837. https://doi.org/10.1016/j.ecoenv.2021.112837.
[71] Zhang, Q., Pardo, M., Rudich, Y., Kaplan-Ashiri, I., Wong, J.P.S., Davis, A.Y., et al., 2019. Chemical composition and toxicity of particles emitted from a consumer-level 3D printer using various materials. Environ Sci Technol 53 (20), 12054–12061. https://doi.org/10.1021/acs.est.9b04168.
[72] Zivkovic, L., Akar, B., Roux, B.M., Spremo Potparevic, B., Bajic, V., Brey, E.M., 2017. Investigation of DNA damage in cells exposed to poly (lactic-co-glycolic acid) microspheres. J Biomed Mater Res A 105 (1), 284–291. https://doi.org/10.1002/jbm.a.35849.